Understanding the Capacity Region of the Greedy Maximal Scheduling Algorithm in Multi-hop Wireless Networks

Changhee Joo, *Member, IEEE*, Xiaojun Lin, *Member, IEEE*, and Ness B. Shroff, *Fellow, IEEE*

Abstract

In this paper, we characterize the performance of an important class of scheduling schemes, called *Greedy Maximal Scheduling* (*GMS*), for multi-hop wireless networks. While a lower bound on the throughput performance of *GMS* has been well known, empirical observations suggest that it is quite loose, and that the performance of *GMS* is often close to optimal. In this paper, we provide a number of new analytic results characterizing the performance limits of *GMS*. We first provide an equivalent characterization of the efficiency ratio of *GMS* through a topological property called the local-pooling factor of the network graph. We then develop an iterative procedure to estimate the local-pooling factor under a large class of network topologies and interference models. We use these results to study the worst-case efficiency ratio of *GMS* on two classes of network topologies. We show how these results can be applied to tree networks to prove that *GMS* achieves the full capacity region in tree networks *under the K-hop interference model*. Then, we show that the worst-case efficiency ratio of *GMS* in geometric unit-disc graphs is between $\frac{1}{6}$ and $\frac{1}{3}$.

I. Introduction

Over the last few years there has been significant interest in studying the *scheduling* problem for multi-hop wireless networks [1]–[8]. In general, this problem involves determining which links should transmit (i.e., which node-pairs should communicate) at what times, what modulation and coding schemes should

C. Joo and N. B. Shroff are with The Ohio State University, e-mail: {cjoo, shroff}@ece.osu.edu

X. Lin is with Purdue University, e-mail: linx@ecn.purdue.edu

This work was supported in part by NSF Awards CNS-0626703, CNS-0721236, ANI-0207728, and CCF-0635202, USA, and in part by IT Scholarship Program supervised by IITA and MIC, Republic of Korea.

A preliminary version of this work was presented at IEEE INFOCOM'08.

be used, and at what power levels should communication take place. While the optimal solution of this scheduling problem has been known for a long time [1], the resultant solution has high computational complexity and is difficult to implement in multi-hop networks. For example, consider the simplest 1-hop interference model (also known as the *node-exclusive* or *primary* interference model), where two links interfere with each other only if they are within a 1-hop distance. Under this model, the throughput-optimal policy of [1] corresponds to a *Maximum Weighted Matching* (*MWM*) policy and its complexity is roughly $O(N^3)$ [9], where N is the total number of nodes in the network. While the 1-hop interference model has been used as a reasonable approximation to Bluetooth or FH-CDMA networks [2], [10], [11], a large class of systems can be modeled using the more general K-hop interference models, in which any two links within a K-hop distance cannot be activated simultaneously. For example, the ubiquitous IEEE 802.11 DCF (Distributed Coordination Function) wireless networks is often modeled using the 2-hop interference model [12], [13], when the carrier-sensing range is equal to the transmission range. On the other hand, when the carrier-sensing range is $(K-1)$ times the transmission range, we can model these networks with K-hop interference models [14]. The complexity of the throughput-optimal policy of [1] for the K-hop interference model is NP-Hard [14], and hence, it is difficult to implement in practice.

In this paper, we are interested in a well-known suboptimal scheduling policy called the *Greedy Maximal Scheduling* (*GMS*) [2], [15] (also known as *Longest Queue First* (*LQF*) in [16], [17]), which determines a schedule by choosing links in a decreasing order of the backlog, while conforming to interference constraints. *GMS* has low complexity [2], [15], [16] and may be implemented in a distributed manner [18]. However, to date its performance is not well-understood. We characterize the performance of *GMS* through its efficiency ratio γ^*, which is defined as the achievable fraction of the optimal capacity region (see Definition 2 for a precise definition). Under the 1-hop interference model, it is relatively straightforward to show that the efficiency ratio of *GMS* is at least $\frac{1}{2}$, i.e., *GMS* can sustain at least a half of the throughput of the optimal policy. However, simulation results suggest that the performance of *GMS* is often much better than this lower bound in most network settings [6]. For the K-hop interference model, the known performance guarantees of *GMS* are also quite pessimistic [12], [14], [19].

Recently, Dimakis and Walrand [17] have shown that if the network topology satisfies the so-called *local-pooling* condition, then *GMS* can in fact achieve the full capacity region. The idea is extended in [20], [21] to find network topologies that maximize the throughput under *GMS*. Unfortunately, realistic network topologies may not satisfy the local-pooling condition. Hence, the true efficiency ratio of *GMS* in many network scenarios remains unknown.

The main objective of this paper is to understand the achievable efficiency ratio of *GMS* for a large class of network topologies and interference models. Understanding the performance limits of *GMS* is important for the following reasons. First, it has been empirically observed in [6] that the centralized *GMS* outperforms many distributed scheduling schemes and achieves virtually the same throughput as the throughput-optimal scheduler for a variety of networking scenarios. Second, although there have been some recently developed distributed scheduling schemes [5], [8] that can achieve the maximum achievable throughput, the study of *GMS* continues to remain attractive because, empirically, *GMS* performs better than these schemes in terms of the resultant queueing delay [3], [6]. Third, it has been known[1] in [18] that *GMS* can be also implemented in a distributed manner, which is critical from the point of view of many multi-hop wireless systems and applications. Finally, recent studies have proposed even simpler constant-time-complexity random algorithms [4], [6], [7] that appear to approximate the performance of *GMS* by giving a larger weight to a link with a larger queue length.

In this paper, we provide a number of new analytical results along this direction. We first generalize the notion of local-pooling in [17] to the notion of the local-pooling factor, which is a topological property of a graph. We show that, under arbitrary interference models, the efficiency ratio of *GMS* for a given network graph is equal to the local-pooling factor of the graph. We then develop an iterative procedure to determine a lower bound on the local-pooling factor of a network graph, and a sufficient condition for a lower bound on the worst-case local-pooling factor over a class of network topologies. We next apply these results to two classes of network topologies. First, we show how these results can be applied to tree networks to prove that *GMS* achieves the full capacity for any tree network under the K-hop interference model. (This result is also shown in [21] by using a different approach.) Second, we develop much sharper bounds on the worst-case efficiency ratio for geometric unit-disc graphs other than those known in the literature.

The rest of the paper is organized as follows. We first describe our system model in Section II. In Section III, we provide an equivalent characterization of the efficiency ratio of *GMS* through the local-pooling factor of the underlying network graph. We develop an iterative analysis method estimating the local-pooling factor of a network graph in Section IV. Using the new methodology, we show that *GMS* achieves the full capacity region in tree topologies under the K-hop interference model in Section V.

[1]Although the distributed algorithm in [18] has been devised to compute matching, it is not difficult to generalize the idea to K-hop interference models. Specifically, we can let each link l decide either to schedule itself or to give up, as follows: Link l will schedule itself if its weight is larger than other interfering links (i.e., links within the K-hop distance from l). Ties can be broken by pre-assigned link IDs. Otherwise, link l will wait until all interfering links with larger weights have decided. If any one of the interfering links with larger weight has been scheduled, link l will give up. If all the interfering links with larger weights have given up, link l schedules itself.

In Section VI, we also provide new results bounding the efficiency ratio of *GMS* in geometric unit-disc graphs. We conclude in Section VII.

II. Network Model

We model a wireless network by a graph $G(V, E, I)$, where V is the set of nodes, E is the set of undirected links, and I represents interference constraints (e.g., an $|E|$x$|E|$ interference matrix). For each link l, let $I(l)$ denote the set of links that interfere with l. For convenience, we adopt the convention that $l \in I(l)$. We define the interference degree $d(l)$ as the maximum number of links in $I(l)$ that do not interfere with each other. We assume a time-slotted system, where the length of each time slot is of unit length. We assume that in each time slot, link l can transmit one packet provided that no other links in $I(l)$ are transmitting at the same time. If two interfering links transmit at the same time, neither of these can transmit any data. This assumption of either collision or perfect reception ignores the possibility of errors due to background noise and also ignores the capture effect [22]. A set of active (i.e., transmitting) links forms a *feasible schedule* in E if none of them interfere with each other. The model is very general representing a large class of wireless networks. For example, in the so-called K-hop interference model, two links within a K-hop "distance" interfere with each other. We can correspondingly define $I(l)$ as, for all links $l \in E$,

$$I(l) = \{k \in E \mid \text{the distance between links } l \text{ and } k \\ \text{is less than or equal to } K \text{ hops}\}.$$

A *maximal schedule* $\vec{M}$ on E is defined as a feasible schedule such that when all links in $\vec{M}$ are activated, no more links can be activated without violating the interference constraints. We use a vector in $\{0,1\}^{|E|}$ to denote a maximal schedule $\vec{M}$ such that the k-th element M_k is set to 1 if link $k \in E$ is included in $\vec{M}$, and to 0 otherwise. Let $\mathcal{M}_E$ be the set of all possible $\vec{M}$'s and let $Co(\mathcal{M}_E)$ denote its convex hull, where the convex hull $Co(A)$ of a set A is defined as

$$Co(A) := \{\textstyle\sum_i w_i \vec{\alpha}_i \mid w_i \geq 0, \sum_i w_i = 1, \vec{\alpha}_i \in A\}.$$

We define a *maximal scheduling vector* $\vec{\phi}$ in E as a vector $\vec{\phi} \in Co(\mathcal{M}_E)$.

We assume that packets arrive at each link l according to a stationary and ergodic process, and that the average arrival rate is λ_l. Further, we assume that the arrival process satisfies the conditions for the fluid limit to hold (e.g., as in [23]). The *capacity region* (or *stability region*) under a given scheduling policy is defined as the set of arrival rate vectors $\vec{\lambda} = \{\lambda_1, \lambda_2, \ldots, \lambda_{|E|}\}$ for which the system is stable (i.e., all queues are kept finite). We define the *optimal* capacity region Λ as the union of the capacity regions of all scheduling policies. The optimal capacity region is known to be,

$$\Lambda = \left\{ \vec{\lambda} \mid \vec{\lambda} \preceq \vec{\phi}, \text{ for some } \vec{\phi} \in Co(\mathcal{M}_E) \right\}, \tag{1}$$

where $\vec{x} \preceq \vec{y}$ denotes that $\vec{x}$ is component-wise dominated by $\vec{y}$. Let $\mathring{\Lambda}$ denote the interior of Λ. This expression can be explained as follows. Assume that $\vec{\lambda} \prec \vec{\phi}$ and $\vec{\phi}$ can be written as a convex combination of vectors in $\mathcal{M}_E$, i.e., $\vec{\phi} = \sum_i w_i \vec{M}_i$, where $w_i \geq 0$ and $\sum_i w_i = 1$. Then by choosing the maximal schedule $\vec{M}_i$ with probability w_i, the service rate at each link will be larger than the arrival rate. Hence the system will be stable. On the other hand, if no vector $\vec{\phi} \in Co(\mathcal{M}_E)$ exists such that $\vec{\lambda} \preceq \vec{\phi}$, then one can show that the system is unstable under any scheduling algorithms [1], [24], [25].

It is well-known that the scheduling policy of [1], which we refer to as the Maximum Weighted Scheduling (*MWS*) policy, achieves the capacity region $\mathring{\Lambda}$. *MWS* chooses a schedule at each time slot t that maximizes the total queue weighted rate sum as

$$\vec{M}^*(t) = \underset{\vec{M} \in \mathcal{M}_E}{\operatorname{argmax}} \sum_{l \in E} q_l(t) M_l,$$

where $q_l(t)$ is the backlog of link l at time t. However, this policy has high computational complexity. The complexity is $O(N^3)$ under the 1-hop interference model and is in general NP-Hard under K-hop interference models ($K \geq 2$). In this paper, we are interested in a suboptimal (but much simpler) policy called *Greedy Maximal Scheduling* (*GMS*) or *Longest Queue First* (*LQF*) policy. *GMS* can be viewed as an approximation to *MWS*. It operates as follows: start with an empty schedule; first pick the link l with the largest backlog; add l into the schedule, and disable other links in $I(l)$; next pick the link l' with the largest backlog from the remaining links, add l' into the schedule, and disable other links in $I(l')$; and this process continues until all links are either chosen or disabled. All chosen links $\{l, l', \cdots\}$ will be scheduled during time slot t. Our goal of the paper is to characterize the efficiency ratio of *GMS* under arbitrary network topologies. The efficiency ratio is defined as follows.

Definition 1: We say that a scheduling policy achieves a *fraction* γ *of the capacity region* under a given network topology if it can keep the system stable for any offered load $\vec{\lambda} \in \gamma\Lambda$, where $0 \leq \gamma \leq 1$.

Definition 2: The *efficiency ratio* $\gamma^*(G)$ of a scheduling policy under a given network graph $G(V, E, I)$ is the supremum of all γ such that the policy can achieve a fraction γ ($0 \leq \gamma \leq 1$) of the capacity region,

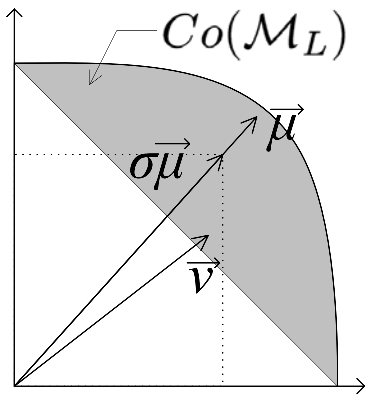

Fig. 1. Given a network graph $G(V, E, I)$, if there exist two vectors $\vec{\mu}, \vec{\nu} \in Co(\mathcal{M}_L)$ for some subset of links $L \subset E$ such that $\sigma\vec{\mu} \succeq \vec{\nu}$, then the graph is said to be σ-dominant.

i.e.,

$$\gamma^*(G) := \sup\{\gamma \mid \text{the system is stable under all offered load vectors } \vec{\lambda} \text{ such that } \vec{\lambda} \preceq \gamma\vec{\phi} \text{ for some } \vec{\phi} \in Co(\mathcal{M}_E)\}. \tag{2}$$

III. An Equivalent Characterization of the Efficiency Ratio of *GMS*

In this section, we provide an equivalent characterization of the efficiency ratio of *GMS* through its topological properties. We start with the following definition.

Definition 3: A graph $G(V, E, I)$ is said to be σ-***dominant***, if there exist two vectors $\vec{\mu}, \vec{\nu} \in Co(\mathcal{M}_L)$ for a subset of links $L \subset E$ such that $\sigma\vec{\mu} \succeq \vec{\nu}$, i.e., $\sigma\mu_i \geq \nu_i$ for all i. The vectors $\vec{\mu}$ and $\vec{\nu}$ are called σ-dominant vectors.

Fig. 1 depicts the convex hull of maximal schedules $Co(\mathcal{M}_L)$ for some subset L and two vectors $\vec{\mu}, \vec{\nu} \in Co(\mathcal{M}_L)$ satisfying that $\sigma\vec{\mu} \succeq \vec{\nu}$. Then the graph G is said to be σ-dominant.

The reason that we are interested in σ-dominance is as follows. Suppose that links in a subset L have larger queues than the rest of the links. Since *GMS* will pick these links first, its service vector will belong to $Co(\mathcal{M}_L)$. However, there is still some uncertainty as to which vector in $Co(\mathcal{M}_L)$ is the actual service vector. It turns out that if there exist two σ-dominant vectors $\vec{\mu}, \vec{\nu} \in Co(\mathcal{M}_L)$ such that $\sigma\vec{\mu} \succeq \vec{\nu}$, then we can construct a traffic pattern that i) has an arrival rate equal to $\sigma\vec{\mu}$ and ii) induces the service vector of *GMS* to be $\vec{\nu}$. (This point is made rigorously in Proposition 1.) Thus the system is unstable at an arrival rate $\sigma\vec{\mu}$, while the arrival rate $\vec{\mu}$ could have been stabilized under a throughput-optimal policy.

Hence, the efficiency ratio of *GMS* will be no greater than σ.

Clearly, if σ is too small, we will no longer be able to find such a subset L and two σ-dominant vectors $\vec{\mu}, \vec{\nu} \in Co(\mathcal{M}_L)$. Intuitively, if we can find the smallest value of σ, for which the graph is σ-dominant, then the smallest value will have some relationship to the efficiency ratio of *GMS*. This notion is reflected in the following definition.

Definition 4: The *local-pooling factor* $\sigma^*(G)$ of a graph $G(V, E, I)$ is the infimum of all σ such that the graph G is σ-dominant. In other words,

$$\begin{aligned} \sigma^*(G) &:= \inf\{\sigma | \ G \text{ is } \sigma\text{-dominant}\} \\ &= \inf\{\sigma | \ \sigma\vec{\mu} \succeq \vec{\nu} \text{ for some } L \text{ and some } \vec{\mu}, \vec{\nu} \in Co(\mathcal{M}_L)\} \\ &= \sup\{\sigma | \ \sigma\vec{\mu} \not\succeq \vec{\nu} \text{ for all } L \text{ and all } \vec{\mu}, \vec{\nu} \in Co(\mathcal{M}_L)\}. \end{aligned} \tag{3}$$

The notion of local-pooling and local-pooling factor was first introduced in [17] and [26], respectively. The definition of *local-pooling* in [17] is equivalent to the definition of a *local-pooling factor of* 1. (We refer to [26] for the details.) It was shown in [17] that, if the local-pooling factor of an arbitrary graph is 1, *GMS* can achieve the efficiency ratio of 1. However, realistic network topologies often do not have a local-pooling factor of 1. In our earlier work [26], we show that under the 1-hop interference model, the efficiency ratio of *GMS* under a given network graph is equivalent to the local-pooling factor of the graph. We next generalize this result to arbitrary interference models.

Proposition 1: The efficiency ratio $\gamma^*(G)$ of *GMS* under a given network graph $G(V, E, I)$ is equal to its local-pooling factor $\sigma^*(G)$.

Remark: Since both $\gamma^*(G)$ and $\sigma^*(G)$ are determined by the network G, in the sequel we will simply use γ^* and σ^* when there is no source of confusion regarding the network G.

The proof of Proposition 1 is a straightforward extension of that of Proposition 8 in [26] and its supporting lemmas. We next sketch the main idea of the proof and refer the readers to [26] for the details. First, as we discuss at the beginning of this section, we can show that $\gamma^* \leq \sigma^*$ by constructing a particular traffic pattern with rate outside $\sigma^*\Lambda$ such that the system is unstable under *GMS*. Specifically, for any $\sigma < \sigma^*$, we can find two σ-dominant vectors $\vec{\mu}, \vec{\nu} \in Co(\mathcal{M}_L)$ satisfying $\sigma\vec{\mu} \succeq \vec{\nu}$. Then for all $\epsilon > 0$, we can construct a traffic pattern with offered load $\vec{\lambda} = \vec{\nu} + \epsilon\vec{e}_L$, under which *GMS* selects the service vector $\vec{\nu}$ on average, where $\vec{e}_L$ is a vector with $e_k = 1$ for $k \in L$ and $e_k = 0$ for $k \notin L$. Thus the system becomes unstable. Since $\vec{\nu} \preceq \sigma\vec{\mu}$, we have $\gamma^* \leq \sigma$ for all $\sigma \leq \sigma^*$. In the other direction, we can obtain $\gamma^* \geq \sigma^*$ by showing that the network is stable under *GMS* for any offered load strictly in $\sigma^*\Lambda$.

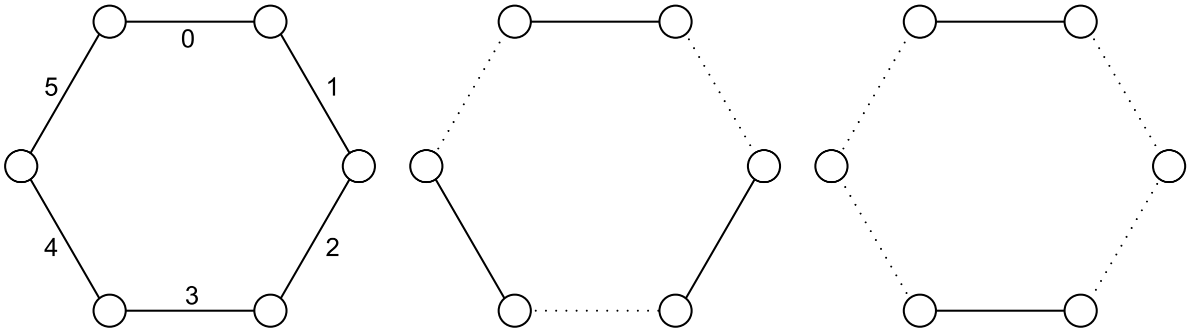

(a) Topology (b) Maximal schedule $\vec{M}_0$ (c) Maximal schedule $\vec{M}_2$

Fig. 2. The 6-link cyclic network and the instances of maximal schedule under the 1-hop interference model. The solid lines in (b) and (c) are the active links.

To elaborate, we can show that in the fluid limit, the longest queue always decreases under *GMS*. To see this, suppose that the set L of links have the longest queue in the fluid limit and they all grow at the same rate $\epsilon > 0$. *GMS* will pick a service rate $\vec{\pi}$ such that $\vec{\pi}|_L \in Co(\mathcal{M}_L)$, where $\cdot|_L$ denotes the projection of a vector onto L. Hence, we have $\vec{\pi}|_L = \vec{\lambda}|_L - \epsilon\vec{e}_L \preceq \vec{\lambda}|_L$. However, since $\vec{\lambda} \in \sigma^* \mathring{\Lambda}$, there must exist a vector $\vec{\phi} \in Co(\mathcal{M}_L)$ such that $\vec{\lambda}|_L \prec \sigma\vec{\phi}$ for some $\sigma < \sigma^*$. Then we obtain that $\vec{\pi}|_L \prec \sigma\vec{\phi}$, which implies that $\vec{\pi}|_L$ and $\vec{\phi}$ are σ-dominant vectors. This contradicts to the definition of the local-pooling factor σ^*. Hence, the longest queue cannot grow. The result of the proposition then follows.

In the following, we further explain the first part of the proof (i.e. $\gamma^* \leq \sigma^*$) using an example. Specifically, we illustrate how, from two σ-dominant maximal scheduling vectors, we can construct a traffic pattern with which the system is unstable under *GMS*. This example will also illustrate how the performance limits of *GMS* are related to maximal scheduling vectors.

Example: We consider the 6-link cyclic network graph under the 1-hop interference model. We illustrate its topology in Fig. 2(a) and number all links clockwise from 0 to 5. All possible maximal schedules under this network graph are listed below.

- $\vec{M}_0 = \{1,0,1,0,1,0\},\ \vec{M}_1 = \{0,1,0,1,0,1\}$,
- $\vec{M}_2 = \{1,0,0,1,0,0\},\ \vec{M}_3 = \{0,0,1,0,0,1\},\ \vec{M}_4 = \{0,1,0,0,1,0\}$.

Note that the number of links included in a maximal schedule is three for $\vec{M}_0$ and $\vec{M}_1$, and is two for $\vec{M}_2$, $\vec{M}_3$, and $\vec{M}_4$. Figs. 2(b) and 2(c) show the two instances of the maximal schedules, i.e., $\vec{M}_0$ and $\vec{M}_2$. Note that we can take two convex combinations $\vec{\mu}, \vec{\nu}$ from maximal schedules (i.e., $\vec{\mu}, \vec{\nu} \in Co(\{\vec{M}_i\})$ as

$$\vec{\mu} = \tfrac{1}{2}\vec{M}_0 + \tfrac{1}{2}\vec{M}_1 = \left\{\tfrac{1}{2}, \tfrac{1}{2}, \tfrac{1}{2}, \tfrac{1}{2}, \tfrac{1}{2}, \tfrac{1}{2}\right\},$$

$$\vec{\nu} = \tfrac{1}{3}\vec{M}_2 + \tfrac{1}{3}\vec{M}_3 + \tfrac{1}{3}\vec{M}_4 = \left\{\tfrac{1}{3}, \tfrac{1}{3}, \tfrac{1}{3}, \tfrac{1}{3}, \tfrac{1}{3}, \tfrac{1}{3}\right\},$$

and hence, $\frac{2}{3}\vec{\mu} \succeq \vec{\nu}$. This implies that the 6-link cyclic network is σ-dominant with $\sigma = \frac{2}{3}$, i.e., its local-pooling factor σ^* must be no larger than $\frac{2}{3}$.

We now show that the efficiency ratio of *GMS* is no larger than $\frac{2}{3}$ by constructing a particular traffic pattern with offered load $\vec{\lambda} = \vec{\nu} + \frac{\epsilon}{3}\vec{e}$ such that the system is unstable under *GMS*, where $\vec{e} = \{1, 1, 1, 1, 1, 1\}$ and ϵ is a small positive number. Assume that all queues in the system are of the same length at time 0.

1) *1st time slot:* One packet is applied to links 0 and 3. Since *GMS* gives priority to links with a longer queue, it will serve links 0 and 3. Therefore, at the end of time slot 1, all queues will still have the same length.
2) *2nd time slot:* One packet is applied to links 1 and 4. For the same reason as above, *GMS* will serve links 1 and 4, and all queues will still have the same length at the end of time slot 2.
3) *3rd time slot:* With probability $1 - \epsilon$, one packet is applied to links 2 and 5. With probability ϵ, two packets are applied to links 2 and 5, and one packet is applied to all other links. In both cases, links 2 and 5 have the longest queue and will be served by *GMS*. At the end of time slot 3, all queues still have the same length. However, with probability ϵ, the queue length increases by 1.

The pattern then repeats itself.

Over all links, the arrival rate is $\frac{1}{3} + \frac{\epsilon}{3}$ and the queue length increases by 1 with probability ϵ every three time slots. Hence, the system with offered load $\vec{\nu} + \frac{\epsilon}{3}\vec{e}$ is unstable under *GMS*. However, the optimal policy (*MWS*) can support an offered load $\vec{\mu} = \frac{3}{2}\vec{\nu}$ in this example. Hence, the efficiency ratio of *GMS* is no greater than $\frac{2}{3}$, i.e., $\gamma^* \leq \frac{2}{3}$ in this 6-link cyclic network under the 1-hop interference model.

Remark: Note that the key in constructing the above traffic pattern is that (i) we keep all queues in L of the same length at all time, (ii) we inject packets according to the maximal schedules that form the vector $\vec{\nu}$ so that these maximal schedules will be picked by *GMS* at all time, and (iii) the offered load is slightly larger than $\vec{\nu}$, i.e., $\vec{\lambda} = \vec{\nu} + \epsilon\vec{e}_L$ so that the queues of L grow to infinity together. In [26], we show that such a traffic pattern can be constructed for all $\vec{\mu}, \vec{\nu}$ such that $\sigma\vec{\mu} \succeq \vec{\nu}$.

Proposition 1 provides an equivalent characterization of the efficiency ratio of *GMS* through the topological properties (i.e., the local-pooling factor) of the given graph. However, it can still be quite difficult to compute the local-pooling factor for an arbitrary network graph. In the next section, we will extend the methodology of Proposition 1 to develop new approaches to estimate the efficiency ratio and the local-pooling factor of arbitrary network graphs.

IV. Estimates of the Local-Pooling Factor for Arbitrary Network Graphs

In this section, we would like to answer the following questions: (i) how do we estimate the local-pooling factor of a given graph? and (ii) what types of graphs will have low local-pooling factors? We now argue that both questions are intimately related to the characterization of a set of unstable links. We first state the following lemma. The proof is provided in Appendix B.

Lemma 1: Given a network graph $G(V,E,I)$ with local-pooling factor σ^*, there exist a subset of links $L \subset E$, and two maximal scheduling vectors $\vec{\mu}^*, \vec{\nu}^* \in Co(\mathcal{M}_L)$ such that $\sigma^* \vec{\mu}^* \succeq \vec{\nu}^*$.

Remark: According to Definition 4, for any $\sigma > \sigma^*$, there exist two σ-dominant vectors $\vec{\mu}, \vec{\nu} \in Co(\mathcal{M}_L)$ such that $\sigma\vec{\mu} \succeq \vec{\nu}$. However, since σ^* is the infimum of such σ, it could be possible that no σ^*-dominant vectors exist in $Co(\mathcal{M}_L)$. Lemma 1 shows that this is not the case.

The idea in the rest of the section is as follows. Suppose that we want to show that $\sigma^* \geq \sigma$ for some $\sigma > 0$. We want to prove by contradiction. Assume in contrary that $\sigma^* < \sigma$. Given a network graph $G(V,E,I)$ with local-pooling factor σ^*, there exist a set $Y \subset E$ and two $\vec{\mu}^*, \vec{\nu}^* \in Co(\mathcal{M}_Y)$ such that $\sigma^* \vec{\mu}^* \succeq \vec{\nu}^*$ from Lemma 1. According to the proof of Proposition 1 (see the example in Section III), we can then construct a traffic pattern with offered load $\vec{\nu}^* + \epsilon\vec{e}_Y$ such that the queues of all links in Y increase to infinity together under *GMS*. Let $\vec{\lambda}^*(\epsilon) = \vec{\nu}^* + \epsilon\vec{e}_Y \in \sigma\mathring{\Lambda}$ denote this offered load[2]. We refer to this set Y as the unstable links. Clearly, if we can show that $Y = \emptyset$, then this leads to a contradiction, which then implies that $\sigma^* \geq \sigma$.

Towards this end, we first study the properties of this set Y of unstable links.

A. *Properties of unstable links*

For a subset $L \subset E$, we let $I_L(l) = I(l) \cap L$ denote the set of links in L that interfere with link l, and define the interference degree $d_L(l)$ as the maximum number of links in $I_L(l)$ that can be scheduled at the same time without interfering with each other. We begin with the following two lemmas.

Lemma 2: If $\vec{\lambda} \in \mathring{\Lambda}$, then $\sum_{j \in I_L(l)} \lambda_j \leq d_L(l)$ for all $l \in L$ and all $L \subset E$.

We note that when $L = E$, Lemma 2 reduces to Lemma 1 in [12]. Lemma 2 is a generalization since the set L can be any subset of E.

Proof: The lemma can be proven by contradiction. We assume that there exist a subset $L \subset E$ and a link $l \in L$ such that $\sum_{j \in I_L(l)} \lambda_j > d_L(l)$. Since $\vec{\lambda}$ is within $\mathring{\Lambda}$, it can be stabilized by some scheduling policy. However, at any time, any schedule must satisfy the interference constraints and thus, cannot serve

[2] Note that there exists some small $\epsilon > 0$ such that $\vec{\lambda}^*(\epsilon) \in \sigma\mathring{\Lambda}$ because $\vec{\nu}^* \in \sigma^*\Lambda \subset \sigma\mathring{\Lambda}$.

more than $d_L(l)$ links out of $I_L(l)$. Hence, the summation of any feasible service rate over $I_L(l)$ cannot exceed $d_L(l)$, which is smaller than the sum of the rates with which packets arrive at $I_L(l)$. Therefore, the network is unstable, which contradicts our assumption. The result of Lemma 2 then follows. ■

Lemma 3: Assume that Y is the set of unstable links under *GMS* with offered load $\vec{\lambda}^*(\epsilon) = \vec{\nu}^* + \epsilon\vec{e}_Y$, then for all $l \in Y$, $\sum_{j\in I_Y(l)} \lambda_j^*(\epsilon) > 1$.

Proof: Note that $\vec{\nu}^* \in Co(\mathcal{M}_Y)$ is a convex combination of elements of $\mathcal{M}_Y$. For each element $\vec{M} \in \mathcal{M}_Y$, if none of the links in $I_Y(l)\backslash\{l\}$ is picked, then l must be picked. Hence, $\sum_{j\in I_Y(l)} M_l \geq 1$. We then have $\sum_{j\in I_Y(l)} \nu_l \geq 1$ and $\sum_{j\in I_Y(l)} \lambda_l^*(\epsilon) > 1$ for all $\epsilon > 0$. ■

Lemma 4: Assume that $\vec{\nu}^* \in \frac{1}{d}\mathring{\Lambda}$ for some $d \geq 1$ and that Y is the corresponding set of unstable links under *GMS*, then for all links $l \in Y$, its interference degree in Y must be larger than d, i.e., $d_Y(l) > d$.

Proof: Again, we prove by contradiction. Suppose that there is a link $l \in Y$ with $d_Y(l) \leq d$. Pick $\vec{\lambda}^*(\epsilon) = \vec{\nu}^* + \epsilon\vec{e}_Y$ such that $\vec{\lambda}^*(\epsilon)$ is strictly within $\frac{1}{d}\Lambda \subset \frac{1}{d_Y(l)}\Lambda$, we have $\sum_{j\in I_Y(l)} \lambda_j^*(\epsilon) \leq 1$ from Lemma 2. However, by Lemma 3, we should have $\sum_{j\in I_Y(l)} \lambda_j^*(\epsilon) > 1$. This is a contradiction. Hence, $d_Y(l)$ must be larger than d. ■

From Lemma 4, we can derive the following main result.

Proposition 2: Given a network graph $G(V, E, I)$, assume that a sequence of links $\{l_1, l_2, \ldots, l_{|E|}\}$ and a sequence of sets $\{L_1, L_2, \ldots, L_{|E|}, L_{|E|+1}\}$ with $L_1 = E$ and $L_{|E|+1} = \emptyset$ satisfy that $L_{i+1} = L_i\backslash\{l_i\}$ and $d_{L_i}(l_i) \leq d$ for all $1 \leq i \leq |E|$ with some $d \geq 1$. Then the local-pooling factor is bounded by $\frac{1}{d}$, i.e., $\sigma^* \geq \frac{1}{d}$.

Proof: We prove the proposition by a contradiction. Suppose that $\sigma^* < \frac{1}{d}$, then there exists $\vec{\mu}^*, \vec{\nu}^* \in Co(\mathcal{M}_Y)$ such that $\sigma^*\vec{\mu}^* \succeq \vec{\nu}^*$. Further, $\vec{\nu}^* \in \frac{1}{d}\mathring{\Lambda}$ since $\sigma^* < \frac{1}{d}$. Let Y denote the corresponding set of unstable links. We now show that Y must be $\emptyset$, which is a contradiction.

If $Y \neq \emptyset$, we can pick the link $l \in Y$ with the smallest index in the set $\{l_1, l_2, \ldots, l_{|E|}\}$, say $l = l_j$. Then we have that all links $l_i \notin Y$ for $1 \leq i < j$ and hence, $Y \subset L_j$. Since $\vec{\nu}^* \in \frac{1}{d}\mathring{\Lambda}$ and $l_j \in Y$, we have $d_Y(l_j) > d$ from Lemma 4. Since we also have $d_Y(l_j) \leq d_{L_j}(l_j)$ from $Y \subset L_j$, and $d_{L_j}(l_j) \leq d$ from our assumption, we arrive at a contradiction and, thus $Y = \emptyset$. ■

Clearly, if there exists a number d such that $d_E(l) \leq d$ for all $l \in E$, then the assumption of Proposition 2 holds for any sequence of links $\{l_1, l_2, \ldots, l_{|E|}\}$. Hence, $\sigma^* \geq \frac{1}{d}$ and the efficiency ratio of *GMS* is no smaller than $\frac{1}{d}$. Note that a similar conclusion has been drawn for Maximal Scheduling. In [12], it has been shown that if $d_E(l) \leq d$ for all $l \in E$, then given $\vec{\lambda} \in \frac{1}{d}\mathring{\Lambda}$, a Maximal Scheduling policy can stabilize the network. However, Proposition 2 is in fact much stronger than the results in [12] and the efficiency ratio of *GMS* can often be shown to be larger than that of Maximal Scheduling. We highlight this important difference with the following example.

Example (Edge Effect): Consider $N+1$ nodes $n_1, n_2, \ldots, n_{N+1}$ lying in a straight line from left to right. Each node is connected only to its immediate neighbors. We denote link (n_i, n_{i+1}) by l_i. Assume the 1-hop interference model. For this network graph, since $d_E(l) \leq 2$ for all links, the efficiency ratio of *GMS* is no smaller than $\frac{1}{2}$. However, *GMS* in fact achieves the full capacity for this graph The reason is that there always exists a link at the end of the line with interference degree of 1. The existence of this link in fact determines the efficiency ratio of *GMS*. To see this, we pick the sequence of links in Proposition 2 as $\{l_1, l_2, \ldots, l_N\}$. We first look at link l_1 on the end of the line. Let $L_1 = E$. Since $d_{L_1}(l_1) = 1$, the assumption of Proposition 2 holds for $i = 2$. Now, we let $L_2 = L_1 \backslash \{l_1\}$ and move our attention to the next link l_2. Since $d_{L_2}(l_2) = 1$, the assumption of Proposition 2 holds for $i = 2$. We can apply this procedure iteratively to links $l_3, l_4, \ldots, l_N$. Therefore, after the N-th iteration, we will have sequences of $\{l_1, l_2, \ldots, l_N\}$ and $\{E = L_1, L_2, \ldots, L_{N+1} = \emptyset\}$ satisfying $L_{i+1} = L_i \backslash \{l_i\}$ and $d_{L_i}(l_i) \leq 1$ for all $1 \leq i \leq N$. Then from Proposition 2, $\sigma^* \geq 1$.

Although the techniques of [17] can also be used to draw the same conclusion that *GMS* achieves full capacity in the simple linear network discussed above, our emphasis here is to illustrate an interesting "edge effect" of *GMS*, which has not been studied in prior works [17], [20], [21]. The example illustrates that the worst-case efficiency ratio of *GMS* depends more on those links with the smallest interference degree. For uniform networks, such links often fall on the edge of the network. Hence, we refer to this property as the "edge effect." However, note that in general such links could also lie in the interior of the network. In the next two sections, we make this intuition rigorous by providing a procedure to derive a lower bound of the efficiency ratio of arbitrary network graphs, and a condition for the worst-case efficiency ratio for a class of graphs.

B. An iterative approach

We present the procedure in Algorithm 1, which bounds the local-pooling factor of the underlying graph, i.e., the efficiency ratio of *GMS*. At each iteration, the algorithm picks up a link and check the interference degree of the chosen link in the remaining network graph.

Let d_e denote the returned value at the end of the algorithm. We show that the local-pooling factor σ^* of the graph $G(V, E, I)$ is at least $\frac{1}{d_e}$.

Lemma 5: Given $G(V, E, I)$, if we obtain d_e from Algorithm 1 with a sequence of $\{l_1, l_2, \ldots, l_{|E|}\}$, then $\sigma^* \geq \frac{1}{d_e}$.

Proof: The lemma directly follows from Proposition 2. Note that the resulting sequence of links

Algorithm 1 Iterative analysis procedure

Initialization: $L_1 \leftarrow E$, $d \leftarrow 1$

1: **for** $1 \leq i \leq |E|$ **do**

2:     Choose a link l_i from L_i

3:     **if** $d_{L_i}(l_i) \geq d$ **then**

4:         $d \leftarrow d_{L_i}(l_i)$

5:     **end if**

6:     $L_{i+1} \leftarrow L_i \backslash \{l_i\}$

7: **end for**

8: **return** d

$\{l_1, l_2, \ldots, l_{|E|}\}$ and the corresponding sequence of sets $\{E = L_1, L_2, \ldots, L_{|E|+1} = \emptyset\}$ satisfy two conditions of $L_{i+1} = L_i \backslash \{l_i\}$ and $d_{L_i}(l_i) \leq d_e$ for all $1 \leq i \leq |E|$. Hence, by Proposition 2, $\sigma^* \geq \frac{1}{d_e}$. ■

The outcome of the algorithm depends on the sequence of links chosen. One possibility is to choose at each iteration i the link with the smallest interference degree in L_i, i.e., in line 2 of Algorithm 1, we choose l_i such that

$$l_i \leftarrow \operatorname*{argmin}_{k \in L_i} d_{L_i}(k). \tag{4}$$

This choice of l_i tends to produce a smaller value of d_e. This procedure can be used to estimate the local-pooling factors of arbitrary network graphs.

It is worth noting that there is some similarity between our iterative procedure and the scheduling algorithms proposed in [19]. Given a network graph, they both order links based on some topological structure of the graph, and tackle the links in the corresponding order. However, they were meant to serve completely different purposes: Algorithm 1 is merely an analytical procedure used to compute the performance bounds of *GMS*. In contrast, the algorithms of [19] are actually used to generate link schedules, and they are not related to *GMS*.

C. The worst-case local-pooling factor over a class of graphs

We are often interested in the worst-case efficiency ratio of a scheduling policy for a class of network graphs. This information is useful when the exact network topology is unknown. Let $\mathbb{P}$ be a set of network graph with certain topological properties and let $\sigma^+(\mathbb{P})$ and $\gamma^+(\mathbb{P})$ denote the worst-case local-pooling factor and the worst-case efficiency ratio, respectively, over all graphs in $\mathbb{P}$, i.e.,

$$\sigma^{+}(\mathbb{P}) := \inf\{\sigma^{*}(G) \mid G \in \mathbb{P}\},$$

$$\gamma^{+}(\mathbb{P}) := \inf\{\gamma^{*}(G) \mid G \in \mathbb{P}\}.$$

We have $\sigma^{+}(\mathbb{P}) = \gamma^{+}(\mathbb{P})$ from Proposition 1.

We next use the methodology of Section IV-B to derive a condition for a lower bound of $\sigma^{+}(\mathbb{P})$. Given $\mathbb{P}$, define $d^{+}(\mathbb{P})$ to be a positive integer with the following property: *For any $G \in \mathbb{P}$, there must exist a link l^{*} such that $d(l^{*}) \leq d^{+}(\mathbb{P})$ and further, $G \backslash \{l^{*}\} \in \mathbb{P}$.* We call $d^{+}(\mathbb{P})$ as the *recurrent interference degree* of $\mathbb{P}$. The following proposition shows that if we can find such a recurrent interference degree $d^{+}(\mathbb{P})$, the worst-case efficiency ratio of *GMS* is bounded by $\frac{1}{d^{+}(\mathbb{P})}$, i.e., $\sigma^{+}(\mathbb{P}) \geq \frac{1}{d^{+}(\mathbb{P})}$.

Proposition 3: Given a network graph $G(V, E, I) \in \mathbb{P}$ with a recurrent interference degree $d^{+}(\mathbb{P})$, the local-pooling factor is bounded by $\sigma^{*}(G) \geq \frac{1}{d^{+}(\mathbb{P})}$.

Proof: Proposition 3 can be proven as Lemma 5. Since $G(V, E, I) \in \mathbb{P}$, there exists link $l_1^{*} \in E$ with $d(l_1^{*}) \leq d^{+}(\mathbb{P})$ and $G \backslash \{l_1^{*}\} \in \mathbb{P}$. Let $L_1 = E$ and $L_2 = E \backslash \{l_1^{*}\}$. Since $G \backslash \{l_1^{*}\} \in \mathbb{P}$, there exists link $l_2^{*} \in L_2$ with $d_{L_2}(l_2^{*}) \leq d^{+}(\mathbb{P})$ and $G \backslash \{l_1^{*}, l_2^{*}\} \in \mathbb{P}$. Repeating this procedure until no link remains, we obtain a sequence of links $\{l_1^{*}, l_2^{*}, \ldots, l_{|E|}^{*}\}$ and a sequence of sets $\{E = L_1, L_2, \ldots, L_{|E|+1} = \emptyset\}$ satisfying $L_{i+1} = L_i \backslash \{l_i^{*}\}$ and $d_{L_i}(l_i^{*}) \leq d^{+}(\mathbb{P})$ for all $1 \leq i \leq |E|$. Hence, from Proposition 2, we conclude that $\sigma^{*}(G) \geq \frac{1}{d^{+}(\mathbb{P})}$. ■

In the following section, we show how to apply Proposition 3 to a class of network graphs.

V. Tree Network Graphs Under the K-hop Interference Model

We first study the efficiency ratio of *GMS* for tree networks. In [17], [20], it has been shown that *GMS* achieves the full capacity in tree networks under the 1-hop interference model. We now show how to use the result in the previous section to prove that *GMS* achieves full capacity for tree network topologies under K-hop interference model. (This result was shown in [21] by using a different approach.) Let $\mathbb{T}^{K}$ be the set of network graphs whose topology forms a tree and the interference relationship is governed by the K-hop interference constraints. Recall that in the K-hop interference model, any two links within a K-hop distance cannot transmit at the same time.

Proposition 4: *GMS* achieves the full capacity for tree networks under the K-hop network model, i.e., $\sigma^{+}(\mathbb{T}^{K}) = 1$.

Proof: It is sufficient to show that $d^{+}(\mathbb{T}^{K}) = 1$ from Proposition 3.

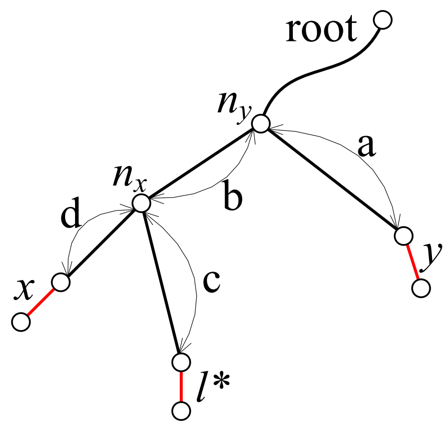

Fig. 3. Tree network graph with the deepest link l^*. Two links $x, y \in I_E(l^*)$ interfere with each other.

Consider a tree network graph $G_t(V, E, I) \in \mathbb{T}^K$. We define the depth of link l in E, denoted by $D(l)$, as the number of hops from link l to the root node of the tree. Let l^* be the link with the largest depth, i.e., $l^* := \text{argmax}_{l \in E} D(l)$. Since l^* is a leaf link of the tree, $G_t \backslash \{l^*\}$ is still a tree, and thus it belongs to $\mathbb{T}^K$.

We next show that the interference degree $d(l^*)$ of link l^* is 1. It suffices to show that any two links $x, y \in I(l^*)$ interfere with each other. Let n_x (or n_y) denote the closest common parent node of x (or y) and l^*. Note that both n_x and n_y lie on the line from link l^* to the root node. Without loss of generality, we assume that n_y is a parent of n_x as shown in Fig. 3. Let a, b, c, and d denote the number of links placed between link y and node n_y, between node n_y and node n_x, between node n_x and link l^*, and between node n_x and link x, respectively. We have the following constraints.

- $a + b + c \leq K - 1$ since link y interferes with link l^*.
- $d \leq c$ since link l^* has the maximum depth.

We thus have $a + b + d \leq K - 1$. In other words, any two links $x, y \in I(l^*)$ interfere with each other, and hence, $d(l^*) = 1$.

In summary, for a graph $G_t(V, E, I) \in \mathbb{T}^K$, there exists a link $l^* \in E$ with the largest depth and its interference degree is $d(l^*) = 1$. Further, $G_t \backslash \{l^*\} \in \mathbb{T}^K$. Therefore, we conclude that $\mathbb{T}^K$ has a recurrent interference degree $d^+(\mathbb{T}^K) = 1$ and the result of Proposition 4 follows. ■

Proposition 4 show that *GMS* is a throughput-optimal scheduling policy in tree networks under K-hop interference models. However, when the network topology is not a tree, in general *GMS* will not have an efficiency ratio of 1. In fact, whenever $K \geq 2$, we can construct network topologies, in which the efficiency ratio of *GMS* can be arbitrarily small under the K-hop interference model. (We refer readers to Appendix A for the construction of these topologies.) As the reader can see in Appendix A, these topologies are somewhat artificial and may not exist in practice. On the other hand, in our prior work [26], we have shown that *GMS* achieves $\frac{\tilde{d}}{2\tilde{d}-1}$ under the 1-hop interference model, where $\tilde{d}$ is the largest node degree of the network graph. This suggests that we may be able to obtain improved bounds on the worst-case performance limits of *GMS* when there are additional constraints on the network topology. Therefore, in the next section, we focus on geometric unit-disc graphs and revisit the question of the worst-case efficiency ratio of *GMS*.

VI. Estimates of the Local-Pooling Factor for Geometric Unit-disc Network Graphs

In this section, we are interested in the performance of *GMS* for undirected unit-disc network graphs, in which the connectivity between nodes and the interference between links depend on their geometric locations. We assume that nodes lie on a finite two-dimensional space. We also assume that two nodes n_i and n_j form a link if their distance $s(n_i, n_j)$ is less than the communication range c, and two links $l_i(n_i^1, n_i^2)$ and $l_j(n_j^1, n_j^2)$ interfere with each other if the distance between any two nodes, one from each pair of nodes $\{n_i^1, n_i^2\}, \{n_j^1, n_j^2\}$, is less than the interference range r. We say that a unit-disc network graph operates under the K-*distance* (interference) model if $r = (K-1)c$, where K is an integer no smaller than 2. Scheduling algorithms for these types of networks have been studied by many researchers, e.g., in [12], [14], [27], [28]. It has been shown that distributed scheduling algorithms can achieve $O(1)$ fraction of the optimal performance. More specifically, Chaporkar *et al.* [12] have shown that the efficiency ratio of Maximal Scheduling is bounded by $\frac{1}{8}$ in arbitrary unit-disc graphs under the 2-distance model, and Sharma *et al.* [14] have shown that it is no smaller than $\frac{1}{49}$ under any K-distance model. In this section, we will show that *GMS* typically has better efficiency ratios than Maximal Scheduling studied in [12], [14].

Our methodology is again based on Proposition 3. Note that the edge links in a unit-disc graph typically have a smaller interference degree than the links in the middle of the graph. If we can bound the interference degree of some edge links l to a number d, we can then use Proposition 3 to show that the efficiency ratio is $\frac{1}{d}$. We will use the methodology first on the 2-distance model, then on K-distance models.

A. *Unit-disc graphs under the* 2*-distance model*

Let $\mathbb{G}_g$ denote the set of graphs conforming to geometric unit-disc constraints. Given a unit-disc network graph $G_g(V, E, I) \in \mathbb{G}_g$, we can assign a two-dimensional coordinate (x, y) for each node. We say that node A is to the left of node B if A's x-coordinate is less than B's x-coordinate. Then for each link l, we can define the left end-point (i.e., node) $n^L(l)$ and right end-point $n^R(l)$. If the two end-points have the same x-coordinate, we assign them to the left or the right arbitrarily. We consider the set of all right nodes of all links $N_V^R = \{n^R(l) \in V \mid l \in E\}$. We say node n in N_V^R is located at the edge if there exist a line through node n such that all other nodes in N_V^R are in the *interior* of one of the half-planes. Note that since the graph is on a two-dimensional finite space, there always exists some right node that is on the edge. Let n_V^R denote the edge node that has the smallest x-coordinate in N_V^R. Then, all other nodes of N_V^R are in the interior of a half-plane (see Fig. 4) whose boundary is through n_V^R. We define a left-most link as a link whose right node is n_V^R. Assuming that every node in V is connected by some links of E (otherwise, we can remove the node from V), we can always find at least one left-most link l^* in E.

Let $\mathbb{G}_g^K$ denote the set of unit-disc network graphs under the K-distance model. The following lemma specifies the performance limits of *GMS* in unit-disc network graphs under the 2-distance model.

Proposition 5: The worst-case efficiency ratio of *GMS* in geometric unit-disc graphs under the 2-distance model is $\frac{1}{6}$, i.e., $\gamma^+(\mathbb{G}_g^2) \geq \frac{1}{6}$.

Sketch of proof: From Proposition 1, it suffices to show that $\sigma^+(\mathbb{G}_g^2) \geq \frac{1}{6}$. Since a unit-disc network graph $G(V, E, I) \in \mathbb{G}_g^2$ has at least one left-most link l^* and $G(V, E, I) \backslash \{l^*\} \in \mathbb{G}_g^2$, it suffices to show that $d(l^*) \leq 6$. It then follows that $\mathbb{G}_g^2$ has a recurrent interference degree $d^+(\mathbb{G}_g^2) \geq 6$, and $\sigma^+(\mathbb{G}_g^2) \leq \frac{1}{6}$ by Proposition 3. We refer the readers to Appendix C for the detailed proof of $d(l^*) \leq 6$. In Fig. 4, we show how 6 links that do not interfere with each other can be placed within the interference range of l^*. In Appendix C, we show that this is the largest number of non-interfering links one can put in $I(l^*)$.

Remark: The key step in the proof of Proposition 3 is to bound the number of neighboring links that can be activated simultaneously. Although the techniques that we used in Appendix C have some similarity to those in [12], in order to improve the bound from 8 (in [12]) to 6, we have to be much more careful in the analysis. Specifically, the left-most link must be carefully chosen (as described above), and more cases of network topology must be considered. For details, please refer to Appendix C.

Recall that Maximal Scheduling achieves an efficiency ratio of $\frac{1}{8}$ in unit-disc graphs under the 2-distance model. Our result shows that with some increase in computational complexity[3], *GMS* indeed outperforms Maximal Scheduling. In the rest section, we show that the performance gap is even bigger for $K > 2$.

[3]The complexity of state-of-the-art distributed *GMS* algorithms [18] is $O(|E|)$, which is higher than that of distributed Maximal Scheduling algorithms [29], which is $O(\log |E|)$.

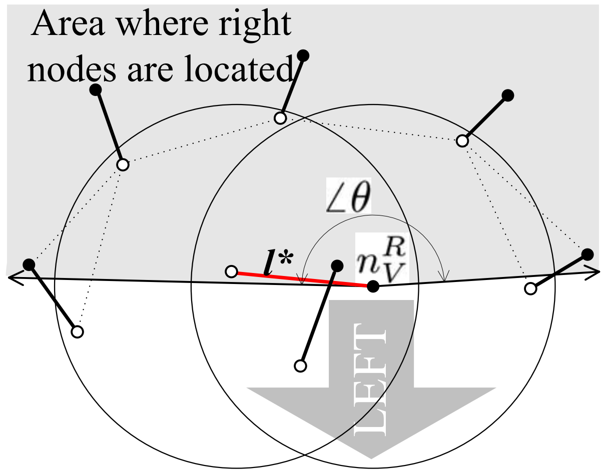

Fig. 4. Geometric network graph under the 2-distance model. Downward is the left direction of the coordinate system as indicated by a big arrow. For each link, its left node is colored in white and its right node in black. The node n_V^R is the left-most right node, the link l^* is the left-most link. Note that all other right nodes must be within an angle of less than 180^o from n_V^R. This figure shows how 6 other links can be placed within the interference range of l^* and they do not interfere with each other. Note that each node of the 6 links must be outside an interference range of c of each other, and further, their right node must be inside an angle less than 180^o from n_V^R.

B. *Unit-disc graphs under K-distance models*

It is well known in the literature that the worst-case efficiency ratio of Maximal Scheduling in unit-disc graphs degrades when K increases [12], [14]. We next show that this is not the case for *GMS*. In fact, the worst-case efficiency ratio of *GMS* tends to increase as K increases. In the next lemma, we compare two graphs $G_1(V, E_1, I) \in \mathbb{G}_g^{K_1}$ and $G_2(V, E_2, I) \in \mathbb{G}_g^{K_2}$ with $K_1 > K_2$. Note that both G_1 and G_2 have the same set of nodes V and have the same interference range r. However, the communication range of G_1 is $c_1 = \frac{r}{K_1 - 1}$, which is smaller than that of G_2, (i.e, $c_2 = \frac{r}{K_2 - 1}$).

Proposition 6: Given a set of nodes V and their location, if $K_1 > K_2$, the local-pooling factor of the network graph $G_1(V, E_1, I) \in \mathbb{G}_g^{K_1}$ is no smaller than the local-pooling factor of the network graph $G_2(V, E_2, I) \in \mathbb{G}_g^{K_2}$, i.e., $\sigma^*(G_1) \geq \sigma^*(G_2)$.

Proof: Note that the set of nodes is the same and the interference range is also identical for both G_1 and G_2. Suppose that we have a subset $L \subset E_1$ in G_1 and two maximal scheduling vectors $\vec{\mu}, \vec{\nu} \in Co(\mathcal{M}_L)$ such that $\sigma\vec{\mu} \succeq \vec{\nu}$. If the same vectors $\vec{\mu}, \vec{\nu}$ are also valid maximal scheduling vectors in G_2, then we have $\sigma^*(G_1) \geq \sigma^*(G_2)$ from the definition of the local-pooling factor. Toward this end, we first show that two maximal scheduling vectors in a subset of links in G_1 are also valid maximal scheduling vectors in G_2.

Since the interference range is fixed, G_1 has a smaller communication range than G_2. Hence, any link in G_1 is also a link in G_2, i.e., $E_1 \subset E_2$. We consider the subset $L \subset E_1$. From $E_1 \subset E_2$, we have $L \subset E_2$. Further, since the interference range is identical, the interference constraints between links in L do not change. Specifically, two links in L that interfere with each other under the K_1-distance model also interfere under the K_2-distance model. Hence, maximal scheduling vectors $\vec{\mu}, \vec{\nu}$ in L under the K_1-distance model are valid maximal scheduling vectors in L under the K_2-distance model.

Therefore, if there exist two maximal scheduling vectors $\vec{\mu}, \vec{\nu} \in Co(\mathcal{M}_L)$ satisfying $\sigma\vec{\mu} \succeq \vec{\nu}$ and a subset L of links in G_1, the same maximal scheduling vectors and the same subset L are valid for G_2. This implies that the local-pooling factor under the K_2-distance model is no greater than σ. Hence, $\sigma^*(G_1) \geq \sigma^*(G_2)$. ■

Remark: Propositions 1 and 6 immediately imply that the efficiency ratio of *GMS* increases as the interference range increases. We note however that this result does not imply that the capacity region of *GMS* increases with K. In fact, as K increases, the optimal capacity region Λ decreases. Hence, the result suggests that as K increases, the optimal capacity region Λ decreases faster than the capacity region of *GMS*. Finally, we note that the result of Proposition 6 is also consistent with the result of [21], which shows that for a given network graph, *GMS* can achieve the optimal capacity region if the interference range K is sufficiently large.

We next state Theorem 1, which is a direct consequence of Propositions 5 and 6.

Theorem 1: The worst-case efficiency ratio of *GMS* in geometric unit-disc graphs under K-distance models is no smaller than $\frac{1}{6}$, i.e., $\gamma^+(\mathbb{G}_g^K) \geq \frac{1}{6}$ for $K \geq 2$.

How tight is this bound? We next present a network graph in $\mathbb{G}_g^K$ with a local-pooling factor of $\frac{1}{3}$.

Lemma 6: There exists a large number K_0 such that for all $K > K_0$ and σ arbitrarily close to $\frac{1}{3}$, some geometric unit-disc graph $G(V, E, I) \in \mathbb{G}_g^K$ has the local-pooling factor no larger than σ, i.e., $\sigma^*(G) \leq \sigma$.

It suffices to construct a graph such that there exists two vectors $\vec{\mu}, \vec{\nu} \in Co(\mathcal{M}_E)$ that satisfy $\sigma\vec{\mu} \succeq \vec{\nu}$. Due to lack of space, we sketch the main idea in this paper. For the detailed proof, we refer the readers to Appendix D.

We construct a network graph $G(V, E, I) \in \mathbb{G}_g^K$ as follows. First, when K is very large, we can think of a link as a point and its interference range as a circle with radius r because the communication range is close to zero. Second, we form two set of links L_1 and L_2. Suppose that $|L_1|$ and $|L_2|$ are finite but very large, and $|L_1| = |L_2|$. Remember that we approximate a link by a point. The links from L_1 form a circle C_1 with radius R at origin O, and links from L_2 form another circle C_2 with radius $R + \frac{\sqrt{3}}{2}r$ at the same origin O. In Fig. 5, we show the small arcs from the two circles. Since the radius R is very large, the two arcs can be approximated by two parallel lines. Since $|L_1|$ and $|L_2|$ are very large, there

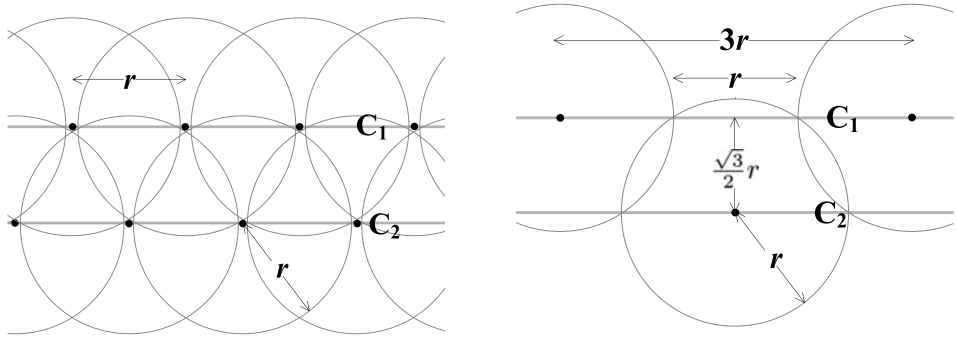

(a) An instance of (dense) maximal schedules $\vec{M}_i$; $\vec{\mu} \in Co(\{\vec{M}_i\})$

(b) An instance of (sparse) maximal schedules $\vec{M}_j$; $\vec{\nu} \in Co(\{\vec{M}_j\})$

Fig. 5. A geometric unit-disc network graph $G(V, E, I) \in \mathbb{G}_g^K$ and $\vec{\mu}, \vec{\nu} \in Co(\mathcal{M}_E)$ such that $\frac{1}{3}\vec{\mu} \succeq \vec{\nu}$. With $K \to \infty$, we assume that a link is a point and its interference range is a circle with radius r. Figures illustrate an instance of maximal schedules from $\vec{\mu}$ and $\vec{\nu}$, respectively. Note that since links are uniformly and closely placed on circles C_1 and C_2 (a small fraction of them is shown in the figures), the interference range of active links in each maximal schedule must cover C_1 and C_2. Let $\vec{\mu}$ consist of dense maximal schedules and let $\vec{\nu}$ consist of sparse maximal schedules. From the uniform placement of (finite) links on C_1 and C_2, the time required to serve all links for a unit time is determined by the distance between two neighboring active links in C_1 (or C_2). Since the distance is r in dense maximal schedules and $3r$ in sparse maximal schedules, we have $\frac{1}{3}\vec{\mu} \succeq \vec{\nu}$.

exists a link at almost every point of the two arcs.

We now find two maximal scheduling vectors $\vec{\mu}, \vec{\nu} \in Co(\mathcal{M}_{L_1 \cup L_2})$. To form $\vec{\mu}$, take any maximal schedules of the form in Fig. 5(a), where active points (i.e., links) are colored in black. Since $|L_1|$ and $|L_2|$ are very large, there will be a large number of such maximal schedules and we produce $\vec{\mu}$ by taking the convex combination with equal weights of these schedules. Similarly, to form $\vec{\nu}$, we take maximal schedules of the form in Fig. 5(b) and produce $\vec{\nu}$ by taking the convex combination with equal weights of them. Clearly, the maximal schedules in Fig. 5(a) are more efficient than those in Fig. 5(b). We next show that the ratio of $\vec{\mu}, \vec{\nu}$ is close to $\frac{1}{3}$.

Assuming that points (i.e., links) are uniformly distributed on C_1 and C_2, then the distance between activated links in Fig. 5(a) is approximately $\frac{1}{3}$ of the distances between activated links in Fig. 5(b). Hence, the schedules that form $\vec{\mu}$ serves 3 times more links than the schedules that form $\vec{\nu}$. We thus obtain that $\frac{1}{3}\vec{\mu}$ is approximately equal to $\vec{\nu}$. Appendix D, we show this with a more formal proof and conclude that $\sigma\vec{\mu} \succeq \vec{\nu}$ with σ close to $\frac{1}{3}$.

Lemma 6 leads to the following corollary.

Corollary 1: There exists a geometric unit-disc network graph $G(V, E, I) \in \mathbb{G}_g^K$ with $K \geq 2$, in which the efficiency ratio of *GMS* is no more than $\frac{1}{3}$.

Proof: From Lemma 6, there exist a number K_0 and graphs $G(V,E,I) \in \mathbb{G}_g^K$ for all $K \geq K_0$ such that $\sigma^*(G) \leq \frac{1}{3}$. By Proposition 6, we also have network graphs $G_K \in \mathbb{G}_g^K$ for all $K \leq K_0$ such that $\sigma(G_K) \leq \sigma(G_{K_0}) \leq \frac{1}{3}$. Therefore, we have $\sigma^+(\mathbb{G}_g^K) \leq \frac{1}{3}$ for all $K \geq 2$. ■

From Theorem 1 and Corollary 1, we can bound the worst-case efficiency ratio of *GMS in arbitrary geometric unit-disc network graphs under the K-distance model* as

$$\frac{1}{6} \leq \gamma^+(\mathbb{G}_g^K) \leq \frac{1}{3}. \quad (5)$$

VII. Conclusion

In this paper, we have provided new analytical results on the achievable performance of *GMS* for a large class of network topologies under general K-hop interference models. We first provide an equivalent characterization of the efficiency ratio of *GMS* through the local-pooling factor of the underlying graph. We then provide an iterative procedure to estimate the local-pooling factor of arbitrary graphs. This new procedure allows us to estimate the worst-case efficiency ratio of *GMS* for a large set of network graphs and interference models. In particular, we observe that *GMS* achieves the optimal capacity region in tree networks *under the K-hop interference model*. Further, in *geometric unit-disc network topologies* under the K-distance interference model, we show that the worst-case efficiency ratio of *GMS* increases with K, and is between $\frac{1}{6}$ and $\frac{1}{3}$.

For future work, there remain many interesting open problems in these directions. For example, it has been empirically shown in [2], [6] that *GMS* achieves the optimal performance in a variety of network settings. This suggests that our bounds on the worst-case efficiency ratio for unit-disc graphs could be further improved. Further, it would be an interesting question whether these results can be extended to interference models other than the geometric unit-disc model, e.g., SNR-based interference model, and non-uniform disc model that incorporates the effects of varying power levels. Finally, we note that there are efforts to develop high-performance scheduling algorithms by ordering links or nodes [19], [30]. It is an interesting direction to explore since, in a certain sense, *GMS* introduces dynamic ordering of links based on the queue lengths.

Appendix

A. Constructing network graphs with arbitrarily small local-pooling factor under the K-hop interference model

While we have shown that *GMS* is a throughput-optimal scheduling policy in tree networks under the K-hop interference model, it is still unclear what are its performance limits in arbitrary network graphs.

We clarify this by carefully constructing some network topologies, in which the efficiency ratio of *GMS* can be arbitrarily small under the K-hop interference model with $K \geq 2$.

We provide a systematic construction of network graphs such that we can find a subset of links L and two maximal scheduling vectors $\vec{\mu}, \vec{\nu} \in Co(\mathcal{M}_L)$ satisfying $\frac{1}{m}\vec{\mu} \succeq \vec{\nu}$ with $m \geq 3$. Once we find those maximal scheduling vectors, we have the upper bound of the efficiency ratio $\gamma^* = \sigma^* \leq \frac{1}{m}$.

Lemma 7: There is a network graph $G^K_{1/m}(V, E, I)$ under the K-hop interference model with $K \geq 2$ such that two vectors $\vec{\mu}, \vec{\nu} \in Co(\mathcal{M}_L)$ with $L \subset E$ satisfies $\frac{1}{m}\vec{\mu} \succeq \vec{\nu}$ for $m \geq 3$

Proof: We start with our systematic construction of a network graph and find two vectors in a subset of links of the constructed network graph. Note that both of them should be a combination of maximal schedules in the subset of links and one must dominate the other by $\frac{1}{m}$.

We construct the network graph $G^K_{1/m}(V, E, I)$ with $K \geq 2$ and $m \geq 3$ as follows:

Phase 1 (horizontal links; see Fig. 6(a) for an example of $K = 2$ and $m = 3$)

1) Start with $N = 2mK$ (or $2m(K+1)$ if K is odd) nodes. Place nodes on a cycle and name them in counter-clockwise order as $\{n^1_1, n^1_2, \ldots, n^1_N\}$. Connect each node n^1_i to its immediate neighbor $n^1_{i\oplus 1}$ for $1 \leq i \leq N$, where $\oplus$ represents a modular addition by $N+1$.
2) Make the circle a centerless wheel by connecting each node n^1_i to the opposite node $n^1_{i\oplus(\frac{N}{2}+1)}$ for $1 \leq i \leq \frac{N}{2}$. All nodes can be connected because N is an even number. Let W^1 denote the constructed wheel graph.
3) Connect n^1_i and $n^1_{i\oplus(K+\lceil\frac{K}{2}\rceil)}$ using $\lfloor\frac{K}{2}\rfloor$-hop links for $1 \leq i \leq N$. That is, for each i, add $(\lfloor\frac{K}{2}\rfloor - 1)$ nodes between n^1_i and $n^1_{i\oplus(K+\lceil\frac{K}{2}\rceil)}$, say $\{\bar{n}_i(1), \bar{n}_i(2), \ldots, \bar{n}_i(\lfloor\frac{K}{2}\rfloor - 1)\}$, and connect them in sequence with links $(\bar{n}_i(k), \bar{n}_i(k+1))$ for $1 \leq k \leq \lfloor\frac{K}{2}\rfloor - 2$. Also, add links $(n^1_i, \bar{n}_i(1))$ and $(\bar{n}_i(\lfloor\frac{K}{2}\rfloor - 1), n^1_{i\oplus(K+\lceil\frac{K}{2}\rceil)})$. If $K = 2$ or 3, connect n^1_i and $n^1_{i\oplus(K+\lceil\frac{K}{2}\rceil)}$ directly.
4) Repeat 3) with n^1_i and $n^1_{i\oplus(jK+\lceil\frac{K}{2}\rceil)}$ for $1 \leq j \leq m-2$.
5) Construct another wheel graph W^K by duplicating W^1, and name nodes on the wheel of W^K accordingly with superscript K.

Phase 2 (vertical links; see Fig. 6(b) for an example of $K = 2$ and $m = 3$)

1) Connect n^1_i and n^K_i using $(K-1)$-hop links for all $1 \leq i \leq N$. That is, for each i, add nodes $\{n^2_i, n^3_i, \ldots, n^{K-1}_i\}$ between n^1_i and n^K_i, and connect them with links (n^k_i, n^{k+1}_i) for $1 \leq k \leq K-1$.
2) Repeat 1) with n^1_i and $n^K_{i\oplus jK}$ for $1 \leq j \leq m-2$.

As an example, all horizontal links and a part of vertical links of $G^2_{1/3}(V, E, I)$ are shown in Fig. 6(a) and Fig. 6(b).

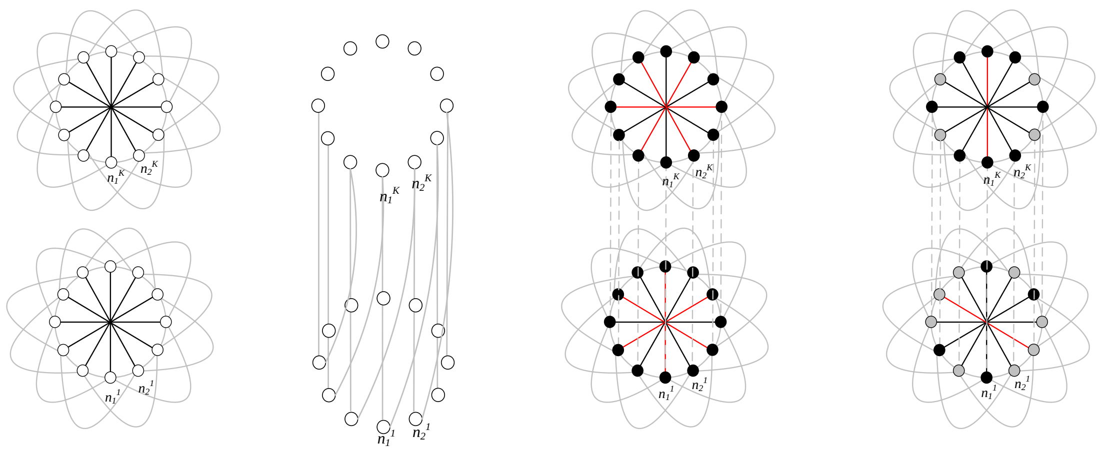

(a) Topology; horizontal links

(b) Topology; a part of vertical links

(c) A maximal schedule of $\vec{\mu}$

(d) A maximal schedule of $\vec{\nu}$

Fig. 6. Example of network graph and schedules of $\gamma = \frac{1}{m}$ under the K-hop interference model with $K = 2$ and $m = 3$. The subset L are the links inside the cycles. (Solid black links in (a).) An instance of maximal schedule for $\vec{\mu}$ is shown in (c). Active links are marked in red. By circulating the active links in (c), we can obtain similar maximal schedules. Assume that $\vec{\mu}$ consists of those maximal schedules with an identical weight. Similarly we can construct $\vec{\nu}$ from maximal schedules like (d). Note that both $\vec{\mu}$ and $\vec{\nu}$ serve all links in L for the same amount of time, but a maximal schedule of $\vec{\mu}$ has 3 times more active links than a maximal schedule of $\vec{\nu}$. Hence, it can be shown that $\vec{\mu}$ dominates $\vec{\nu}$ by $\frac{1}{m}$. To make sure that the schedule of (d) is maximal, we color nodes interfered by the active link in the upper wheel in black, and nodes interfered by the active link in the lower wheel in gray.

Let $L \subset E$ be the set of links *inside* two wheels, i.e., $L = \{(n_i^1, n_{i+\frac{N}{2}}^1), (n_i^K, n_{i+\frac{N}{2}}^K)$ for $1 \le i \le \frac{N}{2}\}$. Let $L^1 = L \cap W^1$ and $L^K = L \cap W^K$. Links in L are presented as solid black lines in Fig. 6(a). Note that links constructed in 3) and 4) of Phase 1 and in 1) and 2) of Phase 2 are designed to control interference among links within and between wheels. If a link l is active in L^1 (or in L^K), then links constructed by 3) and 4) of Phase 1 allows at most $(m-1)$ other links to be active in L^1 (or in L^K). Hence, we can activate at most m links in each wheel (see Fig. 6(c)). However, the inter-wheel interference by vertical links may reduce the number of active links. In 1) and 2) of Phase 2, we have constructed $(m-1)$ vertical links per each node of each wheel. Let $\{l_1^1, l_2^1, \ldots, l_m^1\}$ and $\{l_1^K, l_2^K, \ldots l_m^K\}$ denote links of L^1 and L^K, respectively. If we choose links l_i^1 and l_j^K such that l_i^1 interferes with all links of $L^K \backslash \{l_j^K\}$, and l_j^K interferes with all links of $L^1 \backslash \{l_i^1\}$, then we have only two active links as a maximal schedule in L, i.e., l_i^1 and l_j^K (two red lines in Fig. 6(d)). We design the network graph carefully such that a maximal schedule can include from $2m$ active links to two active links.

Now, we find two convex combinations of maximal schedules in L that one dominates the other by $\frac{1}{m}$.

Consider two sets of maximal schedules; one with maximal schedules of $2m$ active links and the other with maximal schedules of two active links. We first let $\vec{\mu} = \sum_{i=1}^{K} w_i \vec{M}_i$ where $w_i = \frac{1}{K}$ and each maximal schedule $\vec{M}_i$ with $1 \le i \le K$ includes m active links $(n^1_{i \oplus jK}, n^1_{(i+\frac{N}{2}) \oplus jK})$ and $(n^K_{(i+1) \oplus jK}, n^K_{(i+1+\frac{N}{2}) \oplus jK})$ for all $0 \le j \le m-1$. For the other vector, let $\vec{\nu} = \sum_{k=1}^{N/2} v_k \vec{M}_k$ where $v_k = \frac{2}{N}$ and each maximal schedule $\vec{M}_k$ with $1 \le k \le \frac{N}{2}$ includes only two links $(n^1_k, n^1_{k+N/2})$ and $(n^K_{k \oplus (m-1)K}, n^K_{(k+\frac{N}{2}) \oplus (m-1)K})$. Note that $\vec{M}_i$'s and $\vec{M}_k$'s are valid maximal schedules in L. All active links in L are either activated or interfered, and all active links satisfy the interference constraints. Fig. 6(c) and Fig. 6(d) illustrate an instance of $\vec{M}_i$ and $\vec{M}_k$ in $G^2_{1/3}$ respectively. Active links are colored in red. To clearly show the interference in Fig. 6(d), we color a node in black if it is interfered by the active link in the upper wheel, and in gray if it is interfered by the active link in the lower wheel.

Using the scheduling of $\vec{\mu}$ or $\vec{\nu}$, each link in L is served exactly once during a unit time for $\frac{1}{K}$ by $\vec{\mu}$ or for $\frac{2}{N}$ by $\vec{\nu}$. Since $N = 2mK$ (or $2m(K+1)$ if K is odd), we obtain $\frac{1}{m}\mu_l \succeq \nu_l$ for all link $l \in L$ and thus, $\frac{1}{m}\vec{\mu} \succeq \vec{\nu}$. ■

Lemma 7 immediately implies the following proposition.

Proposition 7: Under the K-hop interference model, the efficiency ratio of *GMS* can be arbitrarily small.

Proof: From Lemma 7 and (3), there exists a network graph $G^K_{1/m}(V, E, I)$ with $\sigma^* \le \frac{1}{m}$ for all $K \ge 2$ and $m \ge 3$. Hence, from Proposition 1, *GMS* has $\gamma^* \le \frac{1}{m}$ in the network graph. ■

Proposition 7 lets us know that it is hard, if possible, to characterize the efficiency ratio of *GMS* in arbitrary network graphs under the K-hop interference model.

B. *Proof of Lemma 1*

Assume that $|E|$ is finite. Since for all $L \subset E$, the set of maximal schedules $\mathcal{M}_L$ has finite elements. Then its convex hull $Co(\mathcal{M}_L)$ is bounded and closed, and thus, compact.

By definition of σ^*, for any $k > 0$, there must exist a subset L_k, and two vectors $\vec{\mu}_k, \vec{\nu}_k \in Co(\mathcal{M}_{L_k})$ satisfying $(\sigma^* + \frac{1}{k})\vec{\mu}_k \succeq \vec{\nu}_k$. Hence, we can obtain a sequence $\{(\vec{\mu}_k, \vec{\nu}_k)\}$. Since the number of subsets of E is finite, there must exists a subsequence $(\vec{\mu}_{k_n}, \vec{\nu}_{k_n}) \in Co(\mathcal{M}_L)\text{x}Co(\mathcal{M}_L)$ for some $L \subset E$, where x stands for the cartesian product of the sets. Since $Co(\mathcal{M}_L)$ is a compact set, $Co(\mathcal{M}_L)\text{x}Co(\mathcal{M}_L)$ is compact and hence, $\{(\vec{\mu}_{k_n}, \vec{\nu}_{k_n})\}$ has a convergent subsequence that converges to some element of $Co(\mathcal{M}_L)\text{x}Co(\mathcal{M}_L)$. Let $(\vec{\mu}_{k_i}, \vec{\nu}_{k_i})$ denote the subsequence converging to $(\vec{\mu}^*, \vec{\nu}^*) \in Co(\mathcal{M}_L)\text{x}Co(\mathcal{M}_L)$. Hence, from $(\sigma^* + \frac{1}{k_i})\vec{\mu}_{k_i} \succeq \vec{\nu}_{k_i}$ for all k_i, we obtain $\vec{\mu}^*, \vec{\nu}^* \in Co(\mathcal{M}_L)$ and $\sigma^*\vec{\mu}^* \succeq \vec{\nu}^*$.

C. Proof of Proposition 5

In this section, we prove Proposition 5. Since a geometric unit-disc network graph $G(V, E, I) \in \mathbb{G}_g^2$ has at least one left-most link l^* and $G(V, E, I)\backslash\{l^*\} \in \mathbb{G}_g^2$, it suffices to show that $d(l^*) \leq 6$.

Our strategy is basically to count the number of nodes that can transmit simultaneously in the interference area of l^*: i) We first divide the scenario into cases based on the placement of l^*, i.e., the angle between the link l^* and the y-axis. ii) Then we visit the cases in turn, and in each case, we appropriately partition the interference area of l^* to restrict the number of transmitters in each partition area. iii) Finally, we show that in each case, the total number of nodes that can transmit simultaneously is no greater than 6, i.e., $d(l^*) \leq 6$. To this end, we first provide some definitions following two facts that restrict the number of simultaneous transmitters in a small area. We will use them extensively in the proof.

Fig. 7(a) illustrates the neighborhood of our left-most link l^*. Let L and R denote the location of its left node and right node, respectively. The left direction in the (Cartesian) coordinate system is pointed out by a big gray arrow. The interference area of l^* is a union of two unit disks D_L and D_R with radius r. We assume $r = 1$ for simplicity. Note that the distance[4] between L and R is less than 1, i.e., $\overline{LR} \leq 1$. We divide each disk into 6 equal-size sectors as shown in Fig. 7(a). The points A through J on the edge of the disks denote the boundary of these sectors. Note that in the area where the two disks intersect, some sectors also overlap, and the intersections form triangles. We name these triangles and remaining sectors as P_1 through P_{10}.

We define *indenpendently* interfering nodes or links as follows: Two nodes (or links) are said to *independently* interfere with link l^* if both nodes (or links) interfere with link l^*, but do not interfere with each other. Then, we have the following fact.

- *Fact 1:* If two *independently* interfering nodes are located in the same disk, their angle at the center of the disk should be larger than $\frac{\pi}{3}$ because their distance has to be larger than 1.

Let us define the function $f(\cdot)$ as the number of independently interfering nodes, i.e., if there exists an independently interfering link l_i such that one of its end-point is in P_i, and the other end point is NOT in $\cup_{k=1}^{i-1} P_k$, then we let $f(P_i) = 1$. Otherwise, if there exists no such link l_i, we let $f(P_i) = 0$. Clearly, there is at most one such link l_i for each P_i from Fact 1. If such a link l_i exists, we let N_i to denote the end point in P_i, and $\bar{N}_i$ to denote the other end point. We also define $f(\cdot)$ with multiple arguments as the number of independently interfering nodes in the union of the arguments, i.e., $f(P_i, P_j, P_k) := f(P_i \cup P_j \cup P_k) = f(P_i) + f(P_j \backslash P_i) + f(P_k \backslash \{P_i \cup P_j\})$ for $i < j < k$. If the

[4] Let $\overline{AB}$ denote the distance between two points A and B.

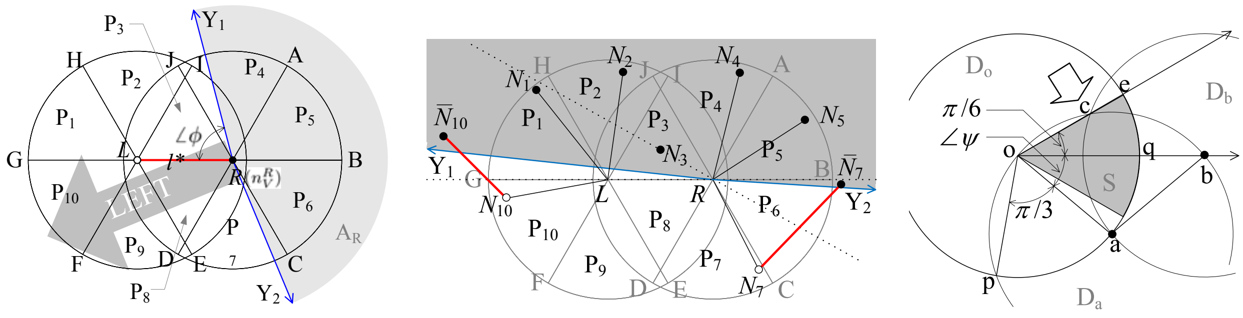

(a) Left-most link l^* and its neighborhood

(b) Diagrams of Case 1 ($0 \leq \phi \leq \frac{\pi}{6}$)

(c) Diagram of Lemma 8

Fig. 7. Neighborhood of the left-most link l^*, and diagrams of Case 1 and Lemma 8.

arguments are mutually exclusive, i.e., for any two arguments X and Y satisfying $X \cap Y = \emptyset$, we have $f(P_i, P_j, P_k) = f(P_i) + f(P_j) + f(P_k)$.

In Fig. 7(a), since R is the position of the left-most right node n_V^R, which is chosen such that all right nodes should be *strictly* inside the right half plane, we can draw two rays Y_1 and Y_2 from R such that all other right nodes are located between these two rays, and the angle $\angle Y_1^* R Y_2^*$ of two rays are less than π, where Y_1^* and Y_2^* are the (infinite) end point of ray Y_1 and Y_2, respectively. We measure an angle clockwise. Let A_R denote the area that other right nodes are located, which is lightly shaded in Fig. 7(a). If an interfering link $l = (N, \bar{N})$ has N not in A_R, the other node $\bar{N}$ should be located in in A_R. In this case, from our choice of the left-most link l^*, N should be a left node, $\bar{N}$ should be a right node, and one of them should be located in $D_L \cup D_R$ (for l to be an interfering link of l^*). The following fact comes from our choice of l^*.

- *Fact 2:* All links interfering with l^* have their right nodes in A_R.

From Fact 2, it is obvious that more (independently interfering) nodes can be located within two disks areas $D_L \cup D_R$ with a larger $\angle Y_1^* R Y_2^*$. In the sequel, we assume that $\angle Y_1^* R Y_2^*$ is very close to π in order to obtain the largest interference degree. Finally, let ϕ denote the angle between Y_1^* and the left-most link l^* as shown in Fig. 7(a). In order to prove Proposition 5, it suffices to show that $d(l^*) \leq 6$ for $0 \leq \phi \leq \frac{\pi}{2}$ because of the symmetry.

1) Case 1: $0 \leq \phi \leq \frac{\pi}{6}$.

Fig. 7(b) illustrates such a case, where a couple of dotted lines indicates two bounds of ϕ. We will first show that $d(l^*) \leq 7$. From $d(l^*) = f(P_1, \ldots, P_{10})$, we have $d(l^*) = f(P_1, P_2, P_4, P_5) + f(P_3, P_8) + f(P_6, P_7) + f(P_9, f_{10})$. Since it is clear that $f(P_1, P_2, P_4, P_5) \leq 4$, we will show in turn that

- $f(P_6, P_7) \leq 1$,
- $f(P_9, P_{10}) \leq 1$,
- $f(P_3, P_8) \leq 1$.

Then we prove that $d(l^*) < 7$ by showing that all the equalities cannot hold at the same time.

We begin with the following lemma and corollary, which will clarify the constraints between independently interfering links, in particularly when one of links has its right node outside $\{D_L \cup D_R\}$.

Lemma 8: For a unit disk D_o at the origin o (see Fig. 7(c)), assume that there are two points a and b: point a is inside D_o and point b is on the positive x-axis. Consider two unit disks D_a and D_b centered at a and b, respectively. If the distance between a and b is less than 1, then the union of two disks includes the shaded sector S of Fig. 7(c), which is the set of points $s \in D_o$ such that $-\frac{\pi}{6} \leq \angle sob \leq \frac{\pi}{6}$.

Proof: If b is within D_o, it is trivial. Hence, we assume that the x-coordinate of b is greater than 1. Let a move on arc of D_o and b is located at the x-axis with distance 1 from a as shown in Fig. 7(c). Clearly, this is the case that the overlap of $D_a \cup D_b$ with D_o is the smallest. Let c denote the point in D_o satisfying $\overline{ca} = \overline{cb} = 1$, which is marked by an arrow in Fig. 7(c).

We represent the coordinate of a by $(\cos\psi, \sin\psi)$, where $\psi := \angle boa$ as shown in Fig. 7(c). Since $\overline{ab} = 1$ and the y-coordinate of b is 0, we can also represent b and c as $b = (2\cos\psi, 0)$ and $c := (c_x, c_y) = (2\cos\psi - \cos(\frac{\pi}{3} - \psi), \sin(\frac{\pi}{3} - \psi))$. Hence, we obtain $c_y = \frac{1}{\sqrt{3}} c_x$. This implies that the point c is on the boundary of S shown in Fig. 7(c). Let e denote the point that line (o, c) meets D_o. Clearly, line segment (o, c) is included in D_a. To conclude that S is included in $D_a \cup D_b$, it suffices to show that line segment (c, e) is included in $D_a \cup D_b$. Since c is already included, we only need to show $e \in D_a \cup D_b$. In the following, we prove by dividing it into three sub-cases.

Note that the coordinate of $e = (\cos\frac{\pi}{6}, \sin\frac{\pi}{6}) = (\frac{\sqrt{3}}{2}, \frac{1}{2})$.

- If $0 \leq \psi \leq \frac{\pi}{6}$, we have $\overline{ae} \leq 1$ and thus $e \in D_a$.
- If $\frac{\pi}{6} < \psi \leq \frac{\pi}{3}$, we have $1 \leq 2\cos\psi < \sqrt{3}$. Hence, we obtain $(\overline{eb})^2 = (\frac{\sqrt{3}}{2} - 2\cos\psi)^2 + \frac{1}{4} \leq 1$, which implies that $e \in D_b$.
- If $\psi > \frac{\pi}{3}$, we have $\overline{eb} \leq 1$ and thus $e \in D_b$.

Therefore, the line segment (c, e) is included in $D_a \cup D_b$, and so is S. ■

Corollary 2: Let p denote the point on the edge of D_o satisfying $\angle aop = \frac{\pi}{3}$, and let q the point where the x-axis meets the edge of D_o as shown in Fig. 7(c). Then, area $(oeqap)$ in D_o is covered by the interference range from the link (a, b).

Proof: We divide the area into three sectors: sectors (oeq), (oqa), and (oap). Sector (oeq) is covered by $D_a \cup D_b$ from Lemma 8. Sector (oqa) is covered by D_a if $0 \leq \psi \leq \frac{\pi}{3}$ and by D_b if $\psi > \frac{\pi}{3}$. Finally, sector (oap) is covered by D_a. ■

We first show $f(P_6, P_7) \leq 1$ by contradiction. We divide A_R into two mutually exclusive areas; $\check{A}_R := \{D_L \cup D_R\} \cap A_R$ and $\hat{A}_R := \{D_L \cup D_R\}^c \cap A_R$. Suppose that $f(P_6, P_7) = 2$. We must have $f(P_7) = 1$, and then $\bar{N}_7 \in \hat{A}_R$ because $N_7 \notin A_R$ and $\bar{N}_7 \notin \cup_{k=1}^{6} P_k$. Since $\angle BR\bar{N}_7 \leq \frac{\pi}{6}$, Corollary 2 (with $a = N_7$ and $b = \bar{N}_7$) immediately implies that sector P_6 is covered by the interference range from link $(N_7, \bar{N}_7)$ as shown in Fig. 7(b). Hence, there cannot be an independently interfering node in P_6, which contradicts our assumption that $f(P_6) = 1$. Similarly, we can show $f(P_9, P_{10}) \leq 1$.

Next, we show $f(P_3, P_8) \leq 1$. Again suppose that $f(P_3, P_8) = 2$, we must have $f(P_8) = 1$, and $\bar{N}_8 \in \hat{A}_R$. Since $\overline{N_8\bar{N}_8} \leq 1$ and $\bar{N}_8 \in \hat{A}_R$, link $l_8 := (N_8, \bar{N}_8)$ should cross either line (L, I) or line (R, J). If the link crosses line (L, I), Corollary 2 (with $a = N_8, b = \bar{N}_8, o = L$) implies that P_3 is covered by the interference range from link l_8. The same conclusion can be drawn if link l_8 crosses line (R, J) by using Corollary 2 with $o = R$. Hence, we obtain $f(P_3) = 0$, which contradicts our assumption that $f(P_3) = 1$.

Then we have

$$f(P_1, \ldots, P_{10}) = f(P_1, P_2, P_4, P_5) + f(P_3, P_8) + f(P_6, P_7) + f(P_9, P_{10}) \leq 7.$$

It remains to show that $d(l^*) < 7$. For notational convenience, let $P_{i,j}$ denote $P_i \cup P_j$. If $f(P_{i,j}) = 1$, we denote the interfering node in $P_{i,j}$ and the other end-point of the corresponding link by $N_{i,j}$ and $\bar{N}_{i,j}$, respectively.

Suppose that $d(l^*) = f(P_1, P_2, P_{3,8}, P_4, P_5, P_{6,7}, P_{9,10}) = 7$. Note that we must have $f(P_1) = f(P_2) = f(P_{3,8}) = \cdots = f(P_{9,10}) = 1$. We are going to prove that this is not possible by showing $\angle Y_1^* LB + \angle GRY_2^* > 2\pi$.

$$\begin{aligned}
&\angle Y_1^* LB + \angle GRY_2^* \\
&= (\angle Y_1^* LN_1 + \angle N_1 LI + \angle ILB) \\
&\qquad + (\angle GRJ + \angle JRN_5 + \angle N_5 RY_2^*) \\
&= \angle Y_1^* LN_1 + \angle N_5 RY_2^* + (\angle N_1 LI + \angle JRN_5) + \tfrac{2\pi}{3}.
\end{aligned}$$

Let us consider each term one by one.

1) We have $\angle Y_1^* LN_1 \geq \angle \bar{N}_{9,10} LN_1 > \frac{\pi}{6}$ from $f(P_{9,10}) = 1$ and Lemma 8.

2) Similarly, we also have $\angle N_5 RY_2^* \geq \angle N_5 R\bar{N}_{6,7} > \frac{\pi}{6}$ from $f(P_{6,7}) = 1$ and Lemma 8.

3) From $\angle N_1LN_2 > \frac{\pi}{3}$, we have $\angle N_1LI + \angle JRN_5 > \frac{\pi}{3} + (\angle N_2LI + \angle JRN_5)$. It is shown[5] in [12] that $(\angle N_2LI + \angle JRN_5) > \frac{2\pi}{3}$. Then, we have $\angle N_1LI + \angle JRN_5 > \pi$.

We then have $\angle Y_1^*LB + \angle GRY_2^* > 2\pi$, which leads to a contradiction because we should have $\angle Y_1^*LB + \angle GRY_2^* < \angle Y_1^*RB + GRY_2^* = \angle GRB + \angle Y_1^*RY_2^* < 2\pi$ from $\angle Y_1^*RY_2^* < \pi$. Hence, we conclude that $f(P_1, P_2, P_{3,8}, P_4, P_5, P_{6,7}, P_{9,10}) < 7$.

2) Case 2: $\frac{\pi}{6} \leq \phi \leq \frac{\pi}{3}$.

We illustrate this case in Fig. 8(a), where we divide $D_L \cup D_R$ into a different partition compared with Case 1. We first describe the new partitions before proceeding with our proof.

Let J' denote the position where ray Y_1 meets the edge of disk D_R. Other points A', B', C' and D' are defined as the points on the edge of disk D_R such that $\angle J'RA' = \angle A'RB' = \angle B'RC' = \angle C'RD' = \frac{\pi}{3}$. Similarly, we set H' as the point where Y_1 meets the edge of disk D_L, and set other points E', F', G', I' on the edge of disk D_L such that $\angle H'LI' = \angle G'LH' = \angle F'LG' = \angle E'LF' = \frac{\pi}{3}$ as shown in Fig. 8(a). We also let K' denote the point where the edges of D_L and D_R meet. Note that since $\overline{LR} \leq 1$, we have $\angle K'LR = \angle LRK' > \frac{\pi}{3}$. Hence, two dotted lines, which present the bounds of $\angle\phi$, go below K'.

We introduce two additional arcs in the figure. Arc (L, R) corresponds to points x between L and R with $\overline{K'x} = 1$ and arc (R, D') corresponds to points x between R and D' with $\overline{C'x} = 1$. We name each area in $D_L \cup D_R$ as follows:

- Q_1: sector $(H'LI')$,
- Q_2: sector $(J'RA')$,
- Q_3: sector $(A'RB')$,
- Q_4: sector $(B'RC')$,
- Q_5^+: the shaded area in $(C'RD')$,
- Q_6^+: the shaded area in the middle including line (L, R),
- Q_8: the shaded sector $(F'LG')$,
- Q_9: sector $(G'LH')$,
- Q_7^+: the remaining area in $D_L \cup D_R$, i.e., area $(F'LRD'E')$, surrounded by shaded areas Q_5^+, Q_6^+, Q_8.

Note that Q_1 and Q_2 are the only two regions that overlap. We define function $f(\cdot)$ and nodes $N_i, \bar{N}_i$ as before using Q_i, i.e., $f(Q_i) = 1$ implies that there exists an independently interfering link such that one end-point $N_i \in Q_i$ and the other end node $\bar{N}_i \notin \cup_{k=1}^{i-1} Q_k$.

[5]If a virtual node N^* is drawn in D_R such that $\angle N_2LB = \angle N^*RB$ and $\overline{N_2L} = \overline{N^*R}$, then it has been proven that $\overline{N^*N_5} > 1$. This implies that $\angle N_2LI + \angle JRN_5 > \frac{2\pi}{3}$. See [12] for the detailed proof.

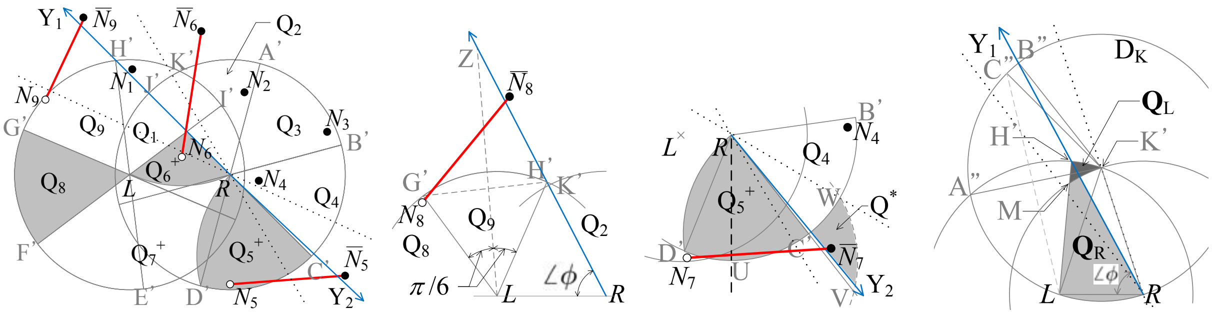

(a) Diagram of Case 2 ($\frac{\pi}{6} \leq \phi \leq \frac{\pi}{3}$)

(b) Diagram of Case 2: Zoomed near sector Q_9

(c) Diagram of Case 2: Areas of Q_5^+ and Q^*

(d) Diagram of Case 3 ($\phi_1 < \phi \leq \frac{\pi}{2}$)

Fig. 8. Diagrams of Cases 2 and 3.

From $d(l^*) = f(Q_1, \ldots, Q_9)$, we will prove $d(l^*) \leq 6$ by showing

- $f(Q_3) \leq 1$,
- $f(Q_8, Q_9) \leq 1$,
- $f(Q_1, Q_2, Q_6^+) \leq 2$,
- $f(Q_4, Q_5^+, Q_7^+) \leq 2$.

Since it is clear that $f(Q_3) \leq 1$, we focus on the rest.

We first show that $f(Q_8, Q_9) \leq 1$. Specifically, we will show that $f(Q_9) = 0$ if $f(Q_8) = 1$. To this end, we show that if $f(Q_8) = 1$, then $\angle \bar{N}_8 L H' \leq \frac{\pi}{6}$. Then using Corollary 2 (with $a = N_8, b = \bar{N}_8, o = L$), we can conclude that $f(Q_9) = 0$. In the following, we prove that $\angle \bar{N}_8 L H' \leq \frac{\pi}{6}$ when $\phi \leq \frac{\pi}{3}$.

Let us consider area Q_9 in detail. Fig. 8(b) illustrates the zoomed diagram. Let Z denote the point on Y_1 satisfying $\angle ZLH' = \angle G'LZ = \frac{\pi}{6}$. Clearly, if link $(N_8, \bar{N}_8)$ crosses line segment (Z, H'), we have $\angle \bar{N}_8 L H' \leq \frac{\pi}{6}$. We are going to show that G' is the closest point in Q_8 to Z, and that $\overline{G'Z} \geq 1$. Then from $\overline{N_8 \bar{N}_8} \leq 1$ and $N_8 \in Q_8$, link $(N_8, \bar{N}_8)$ should cross line segment (Z, H').

Note that we have $\overline{LR} \leq 1$, $\overline{LH'} = 1$, and $\overline{H'R} \geq 1$, which imply that $\angle RH'L \leq \frac{\pi}{3}$. Then, from $\angle LH'G' = \frac{\pi}{3}$, $\overline{G'H'} = 1$, and the fact that lines (G', H') and (L, Z) are perpendicular, it follows that $\overline{LZ} \geq \sqrt{3}$. Since $\angle G'LZ = \frac{\pi}{6}$, we have $\overline{LZ}(\cos \angle G'LZ) > 1 = \overline{G'L}$, and conclude that G' is the closest point in Q_8 to Z. Hence, it suffices to show $\overline{G'Z} \geq 1$.

Since $\angle RH'L \leq \frac{\pi}{3}$, it follows $\angle H'ZL = \angle RH'L - \angle ZLH' \leq \frac{\pi}{6}$. From $\angle H'ZL \leq \frac{\pi}{6} = \angle ZLH'$, we obtain $\overline{H'Z} \geq \overline{H'L} = 1$. Therefore, we conclude $\overline{G'Z} = \overline{H'Z} \geq 1$, which results in $f(Q_9) = 0$ from Corollary 2, and we have $f(Q_8, Q_9) \leq 1$.

Next, we prove $f(Q_1, Q_2, Q_6^+) \leq 2$ using the following lemmas.

Lemma 9: If three nodes x, y, z satisfy that $\overline{xz} \leq 1$ and $\overline{yz} \leq 1$, then all points t in triangle area (xyz) satisfy $\overline{xt} \leq 1$ or $\overline{yt} \leq 1$.

Lemma 9 is obvious and we omit the proof.

Lemma 10: If two nodes x and y satisfy $\overline{xy} \leq \sqrt{3}$, and link $l = (a, b)$ with $\overline{ab} \leq 1$ intersects line segment (x, y), then the link interferes with either x or y.

We also omit the proof of Lemma 10. It can be easily shown by drawing two nodes x, y with $\overline{xy} \leq \sqrt{3}$ and a link (a, b) with $\overline{ab} \leq 1$. From $\overline{ab} \leq 1$ and $\overline{xy} \leq \sqrt{3}$, we should have $\overline{ax} \leq 1$, $\overline{ay} \leq 1$, $\overline{bx} \leq 1$, or $\overline{by} \leq 1$.

We prove $f(Q_1, Q_2, Q_6^+) \leq 2$ by contradiction. Supposing $f(Q_1, Q_2, Q_6^+) = 3$, we must have $f(Q_1) = f(Q_2) = f(Q_6^+) = 1$. Note that $Q_6^+ \cap A_R = \emptyset$. Then, $f(Q_6^+) = 1$ implies that there must exists $\bar{N}_6 \in \hat{A}_R$. Note that link $l_6 := (N_6, \bar{N}_6)$ will divide Q_1 or Q_2 (or both of them) into two parts. If it divides Q_1 (or Q_2, correspondingly), from Corollary 2 node N_1 cannot be in the right part of Q_1 (or node N_2 cannot be in the left part of Q_2, correspondingly). This implies that link l_6 intersects either line segment (N_1, K') or (N_2, K'). Moreover, since $\overline{N_1K'} \leq 1$ and $\overline{N_2K'} \leq 1$, from Lemma 9 node N_6 cannot be in the triangle area of (N_1N_2K'). This immediately implies that N_6 should be located below line segment (N_1, N_2). Hence link l_6 must intersect line segment (N_1, N_2). Now we use Lemma 10 to prove that this is not possible. In the following, we show that the distance between any two points within $Q_1 \cup Q_2$ is no greater than $\sqrt{3}$ (i.e., $\overline{N_1N_2} \leq \sqrt{3}$). Then, Lemma 10 implies that independently interfering link l_6 cannot exist, i.e., $f(Q_6^+) = 0$.

It is easy to see that $\max_{X \in Q_1, Y \in Q_2} \overline{XY}$ is equal[6] to $\max\{1, \overline{H'R}, \overline{LA'}, \overline{H'A'}\}$. We can show that each length is no greater than $\sqrt{3}$.

1) First we consider $\overline{H'R}$. Let $\theta := \angle H'LR$, and let the coordinate of L to be $(0, 0)$. Then we have $H' = (\cos\theta, \sin\theta)$, $R = (\overline{LR}, 0)$, and $\overline{H'R}^2 = (\overline{LR} - \cos\theta)^2 + \sin^2\theta = \overline{LR}^2 - 2\overline{LR}\cos\theta + 1$. Using $\cos\theta = \overline{LR} - \overline{H'R}\cos\phi$, we obtain $\overline{H'R}^2 - (2\overline{LR}\cos\phi)\overline{H'R} + \overline{LR}^2 - 1 = 0$. Hence, we have $\overline{H'R} = \overline{LR}\cos\phi + \sqrt{\overline{LR}^2\cos^2\phi + (1 - \overline{LR}^2)}$. Note that $\overline{H'R}$ is decreasing in ϕ for $\frac{\pi}{6} \leq \phi \leq \frac{\pi}{3}$ since $\cos\phi$ is decreasing. Hence, by setting $\phi = \frac{\pi}{6}$, we can maximize $\overline{H'R}$, and obtain $\overline{H'R} = \frac{\sqrt{3}}{2}\overline{LR} + \sqrt{1 - \frac{1}{4}\overline{LR}^2}$. Differentiating with respect to $\overline{LR}$, we have $\frac{d}{dLR}\overline{H'R} > 0$ because $\frac{d}{dLR}\sqrt{1 - \frac{1}{4}\overline{LR}^2} \geq -\frac{1}{2\sqrt{3}}$ for $0 \leq \overline{LR} \leq 1$. Therefore, we obtain $\overline{H'R} \leq \sqrt{3}$ where the equality holds when $\phi = \frac{\pi}{6}$ and $\overline{LR} = 1$.

[6] For a point $x \in Q_1$, let D_1 and D_2 denote two disks centered at x with radius $\max\{1, \overline{xR}\}$ and $\max\{1, \overline{xA'}\}$ respectively. Then, clearly $Q_2 \subset D_1 \cup D_2$, and thus $\overline{xY} \leq \max\{1, \overline{xR}, \overline{xA'}\}$ for all $Y \in Q_2$. Similarly, for a point $y \in Q_2$, we have $\overline{Xy} \leq \max\{1, \overline{Ly}, \overline{H'y}\}$ for all $X \in Q_1$. Therefore, we obtain $\max_{X \in Q_1, Y \in Q_2} \overline{XY} = \max\{1, \overline{H'R}, \overline{LA'}, \overline{H'A'}\}$.

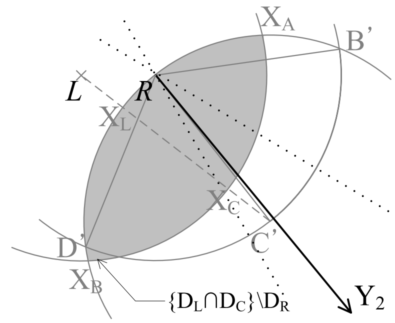

Fig. 9. Zoomed diagram of Case 2; Area of $\{D_L \cap D_C\}$

2) Next we consider $\overline{LA'}$. Let the coordinate of R to be $(0,0)$. We have $L = (-\overline{LR}, 0)$, $A' = (\cos(\frac{2\pi}{3} - \phi), \sin(\frac{2\pi}{3} - \phi))$, and thus $\overline{LA'}^2 = \overline{LR}^2 + 2\overline{LR}\cos(\frac{2\pi}{3} - \phi) + 1$. Clearly it is increasing in $\overline{LR}$ for $\frac{\pi}{6} \leq \phi \leq \frac{\pi}{3}$. So by setting $\overline{LR} = 1$, we can maximize $\overline{LA'}$, and obtain $\overline{LA'}^2 = 2 + 2\cos(\frac{2\pi}{3} - \phi) \leq 3$ from $0 \leq \cos(\frac{2\pi}{3} - \phi) \leq \frac{1}{2}$.

3) Finally, $\overline{H'A'} \leq \overline{H'J'} + \overline{J'A'} \leq (\overline{H'R} - \overline{J'R}) + 1 \leq \sqrt{3}$.

Hence, we obtain $\max_{X \in Q_1, Y \in Q_2} \overline{XY} \leq \sqrt{3}$, which immediately implies that $\overline{N_1N_2} \leq \sqrt{3}$. From Lemma 10, it leads to $f(Q_6^+) = 0$, which contradicts our assumption that $f(Q_1, Q_2, Q_6^+) = 3$ and we conclude $f(Q_1, Q_2, Q_6^+) \leq 2$.

Finally, we show $f(Q_4, Q_5^+, Q_7^+) \leq 2$. To begin with, we note that if $f(Q_7^+) \geq 1$, an interfering link must cross ray Y_2. The link cannot pass through Y_1 to reach $\check{A}_R$ because its distance would have been larger than 1. However, there can be a link $l_7 := (N_7, \bar{N}_7)$ crossing Y_2 as shown in Fig. 8(c). We first show that there is at most one such link, i.e., $f(Q_7^+) \leq 1$.

Fig. 8(c) illustrates a scenario with $f(Q_7^+) = 1$. Let U denote a point on the edge of D_R with $\angle URL = \frac{\pi}{2}$. Let the coordinate of R be $(0,0)$, then the coordinate of U is $(0,-1)$, and clearly node N_7 has its coordination (n_x, n_y) with $n_x \leq 0$ and $n_y \geq -1$. Let V denote the point on the extension of line (R, C') satisfying $\overline{UV} = 1$ and let W denote the point on the edge of D_R with $\overline{UW} = 1$, as shown in the figure. Points v with $\overline{Uv} = 1$ are drawn as a dashed arc. The points V and W are where the extended line (R, C') and the disk D_R, respectively, meet the dashed arc. Since N_7 has $n_x \leq 0$ and $n_y \geq -1$, its other end node $\bar{N}_7$ should be located in the area i) above line (C', V), ii) within the dashed arc centered at U, and iii) the exterior of D_R. Let Q^* denote this area as shown in Fig. 8(c).

Let D_C denote a unit disk centered at C' (part of D_C overlaps with the shaded area in Fig. 8(c)). Note that if $f(Q_7^+) \geq 1$, we have $N_7 \in Q_7^+$ and $\bar{N}_7 \in Q^*$, and it is clear that $\overline{N_7C'} \leq 1$, i.e., C' is the closest point[7] in Q^* to Q_7^+. Then, node $N_7 \in Q_7^+$ should be located within the area $\{D_C \cap D_L\} \backslash D_R$. Let X_A and X_B denote the point where D_C and D_L meet above and below line (L, C'), respectively, and also let X_L and X_C denote the point where line segment (L, C') meets D_L and D_C, respectively. We divide $D_C \cap D_L$, which is the shaded area in Fig 9, into two areas $(X_A X_L X_C)$ and $(X_B X_L X_C)$. Since $\overline{LR} \le 1$ and $\overline{RC'} = 1$, R is located on arc (X_L, X_A), which implies that D_R includes area $(X_A X_L X_C)$ because $\overline{LC'} \ge 1$. Hence, it follows that area $(X_B X_L X_C)$ includes $\{D_C \cap D_L\} \backslash D_R$. Again from $\overline{LC'} \ge 1$, it is easy to see that any two points within area $(X_B X_L X_C)$ has a distance less than 1. Therefore, we obtain $f(Q_7^+) = f(Q_7^+ \cap \{D_C \cap D_L\} \backslash D_R) \le 1$.

Now we prove $f(Q_4, Q_5^+, Q_7^+) \le 2$ by contradiction. Suppose $f(Q_4, Q_5^+, Q_7^+) = 3$. Since each area can hold only one independently interfering node, we must have $f(Q_4) = 1$, $f(Q_5^+) = 1$ and $f(Q_7^+) = 1$. We prove that this is not possible by showing $f(Q_5^+) = 0$ when $f(Q_4) = 1$ and $f(Q_7^+) = 1$.

Let us consider a scenario with $f(Q_4) = 1$ and $f(Q_7^+) = 1$ as shown in Fig. 8(c). Note that link $l_5 := (N_5, \bar{N}_5)$ and l_7 cannot intersect with each other from Lemma 10, and the interference range from link l_7 covers lower part of Q_5^+. Hence, link l_5 can only be placed above link l_7. Link l_5 also has to go below N_4 (i.e., cannot cross line segment (R, N_4)) because otherwise we should have $f(Q_4) = 0$ from Corollary 2, which contradicts our assumption that $f(Q_4) = 1$. Also note that $\bar{N}_5 \notin Q_4$ and $\bar{N}_5 \notin Q^*$ due to the interference range from N_4 and $\bar{N}_7$ respectively, and $\bar{N}_5 \notin$ triangle area of $(N_4 \bar{N}_7 C')$ from Lemma 9. These along with the facts that link l_5 goes below (R, N_4) and above l_7 imply that $\bar{N}_5$ cannot be located to the left of line $(N_4, \bar{N}_7)$ and hence, link l_5 must intersect line segment $(N_4, \bar{N}_7)$.

It remains to show that $\overline{XY} \le \sqrt{3}$ for all $X \in Q_4$ and $Y \in Q^*$, which implies that $\overline{N_4 \bar{N}_7} \le \sqrt{3}$. Then from Lemma 10, any link intersecting line segment $(N_4, \bar{N}_7)$ will interfere with either N_4 or $\bar{N}_7$, which will lead to $f(Q_5^+) = 0$. From Fig. 8(c), it is clear that $\max_{X \in Q_4, Y \in Q^*} \overline{XY} < \max\{\overline{RV}, \overline{B'V}\}$ when $\frac{2\pi}{3} \le (\angle VRL = \pi - \phi) \le \frac{5\pi}{6}$. From $\overline{RU} = 1$, $\overline{UV} = 1$ and $\angle VRU \ge \frac{\pi}{6}$, we have $\overline{RV} \le \sqrt{3}$. Moreover, from $\overline{RB'} = 1$, $\angle B'RV = \frac{\pi}{3}$ and $\overline{RV} \le \sqrt{3}$, we also have $\overline{B'V} < \sqrt{3}$. Hence, we conclude that $\max_{X \in Q_4, Y \in Q^*} \overline{XY} \le \sqrt{3}$, and $\overline{N_4 \bar{N}_7} \le \sqrt{3}$.

Summing up all results, we obtain $d(l^*) \le f(Q_3) + f(Q_8, Q_9) + f(Q_1, Q_2, Q_6^+) + f(Q_4, Q_5^+, Q_7^+) \le 6$.

3) Case 3: $\frac{\pi}{3} < \phi \le \phi_1$, where $\phi_1 := \angle LRK'$ in Fig. 8(d).

Using the same partitioning approach and the techniques as in Case 2, we can show the following.

- $f(Q_3) \le 1$.
- $f(Q_8, Q_9) \le 1$: To prove this, we need $\angle RH'L \le \frac{\pi}{3}$, which comes from $\overline{LR} \le 1$, $\overline{LH'} = 1$, and

[7]It can be shown from the fact that the closest point on Y_2 to $N_7 \in Q_7^+$ is on line segment (R, C').

$\overline{H'R} \geq 1$.

- $f(Q_1, Q_2, Q_6^+) \leq 2$: To prove this, we need to show that $\overline{H'R} \leq \sqrt{3}$ and $\overline{LA'} \leq \sqrt{3}$. For $\overline{H'R} \leq \sqrt{3}$, we can use the same approach as in Case 2 and the result is straightforward. For $\overline{LA'} \leq \sqrt{3}$, we begin with $\overline{LA'}^2 = \overline{LR}^2 + 2\overline{LR}\cos(\frac{2\pi}{3} - \phi) + 1$. Since $\overline{LA'}^2$ is increasing in ϕ for $\frac{\pi}{3} \leq \phi \leq \phi_1 \leq \frac{\pi}{2}$, we can maximize $\overline{LA'}^2$ with $\phi = \phi_1$. Since $\cos\phi_1 = \frac{1}{2}\overline{LR}$, we have $\overline{LA'}^2 = \frac{1}{2}\overline{LR}^2 + \overline{LR}\sqrt{3 - \frac{3}{4}\overline{LR}^2} + 1$. We can verify that it is increasing in $\overline{LR} \leq 1$. Hence, we obtain $\overline{LA'}^2 \leq 3$ where the equality holds with $\overline{LR} = 1$ and $\phi = \phi_1$.
- $f(Q_7^+) \leq 1$, and thus $f(Q_4, Q_5^+, Q_7^+) \leq 3$.

Then we prove that $d(l^*) \leq 6$ by showing that for the above equations, the equalities cannot hold all at the same time.

Suppose that $d(l^*) = 7$. Clearly, we must have $f(Q_3) = 1, f(Q_8, Q_9) = 1, f(Q_1, Q_2, Q_6^+) = 2, f(Q_4, Q_5^+, Q_7^+) = 3$. Let $l_{8,9} := (N_{8,9}, \bar{N}_{8,9})$ denote the independently interfering link in $Q_8 \cup Q_9$. Also let $\mathbf{Q}_L := Q_1 \backslash D_R$ and $\mathbf{Q}_R := \{Q_1 \cup Q_2 \cup Q_6^+\} \backslash \{Q_2 \cup \mathbf{Q}_L\}$, which are presented as dimly and lightly shaded areas, respectively, in Fig. 8(d). The two dotted lines are the bounds of ϕ. We will show that the interference range from $l_{8,9}$ covers $\mathbf{Q}_L$. Once the interference range from link $l_{8,9}$ includes $\mathbf{Q}_L$, we must have $f(Q_2) = 1$ and $f(\mathbf{Q}_R) = 1$ from $f(Q_1, Q_2, Q_6^+) = 2$, it follows $f(\mathbf{Q}_R, Q_2, Q_3, Q_4, Q_5^+) = 5$. However, this leads to contradiction to $Y_1^* R Y_2^* < \pi$. Let $\mathbf{N}_R$ denote the independently interfering node in $\mathbf{Q}_R$, and let $\bar{\mathbf{N}}_R$ denote the corresponding other end-point. Since $\mathbf{N}_R \notin A_R$, we must have $\bar{\mathbf{N}}_R \in \hat{A}_R$, and thus we obtain

$$\begin{aligned}\angle Y_1^* R Y_2^* &\geq \angle \bar{\mathbf{N}}_R R N_2 + \angle N_2 R N_4 + \angle N_4 R \bar{N}_5 \\ &> \tfrac{\pi}{6} + \tfrac{2\pi}{3} + \tfrac{\pi}{6} = \pi,\end{aligned}$$

from Lemma 8 and Fact 1. Then, we can conclude that $d(l^*) \leq 6$.

In the following, we show that the interference range from link $l_{8,9}$ includes $\mathbf{Q}_L$. We first prove that K' is included in the interference range. Let M denote the point where disk D_R meets line segment (H', L) as shown in Fig. 8(d). Let D_K denote a unit disk centered at K', and let A'' and B'' denote the point where D_K meets D_L and Y_1 respectively as shown in Fig. 8(d). Note that if $\angle A''K'B'' \geq \frac{\pi}{3}$, then the interference range from $l_{8,9}$ includes K': To see this, note that if $N_{8,9} \in D_K$, then $\overline{K'N_{8,9}} \leq 1$, i.e., K' is covered by interference range from $N_{8,9}$. On the other hand, if $N_{8,9} \notin D_K$, we must have $\bar{N}_{8,9} \in D_R$, because otherwise we arrive at a contradiction that $\overline{N_{8,9}\bar{N}_{8,9}} > \overline{A''B''} \geq 1$. Hence, K' is then covered by the interference range of $\bar{N}_{8,9}$, and $\overline{K'\bar{N}_{8,9}} \leq 1$. Now let $\eta = \angle K'B''R = \angle B''RK'$.

We have

$$\angle A''K'B'' = \angle RK'B'' - \angle LK'A'' - \angle RK'L$$

$$= (\pi - 2\eta) - \tfrac{\pi}{3} - (\pi - 2(\phi + \eta)) \geq \tfrac{\pi}{3}.$$

The last inequality comes from $\phi \geq \frac{\pi}{3}$. Hence, the interference range from $l_{8,9}$ includes K', i.e., $\overline{K'N_{8,9}} \leq 1$ or $\overline{K'\bar{N}_{8,9}} \leq 1$.

If $\overline{K'N_{8,9}} \leq 1$, node $N_{8,9}$ is within sector $(K'LA'')$ of D_K, which implies that $\mathbf{Q}_L$ is included in the interference range from $N_{8,9}$. If $\overline{K'N_{8,9}} > 1$, we must have $\overline{K'\bar{N}_{8,9}} \leq 1$, and then node $\bar{N}_{8,9}$ is located within D_K and on the right side of Y_1. Let C'' a point on D_K satisfying $\overline{A''C''} = 1$ as shown in Fig. 8(d). Note that C'' is on the left of B'' from $\angle A''K'B'' \geq \frac{\pi}{3}$, and that $\angle A''LC'' = \angle C''LK' = \frac{\pi}{6}$. Then, it is clear that link $l_{8,9}$ crosses line segment (C'', L), which implies that $\angle \bar{N}_{8,9}LK' \leq \angle C''LK' = \frac{\pi}{6}$. Then, from Corollary 2, line (L, K') is included in the interference range from $l_{8,9}$ and so is $\mathbf{Q}_L$.

Therefore, we have $f(Q_2) = 1$ and $f(\mathbf{Q}_R) = 1$. Since $f(\mathbf{Q}_R, Q_2, Q_3, Q_4, Q_5^+) = 5$ contradicts our assumption, we conclude that $d(l^*) \leq 6$.

4) Case 4: $\phi_1 < \phi \leq \frac{\pi}{2}$.

The procedure is similar as in Case 3. We partition the interference area of l^* such that the interference constraints lead to multiple inequalities, and show that all the equalities cannot hold at the same time. We first describe the partition and proceed with the proof.

This case is depicted in Fig. 10. Again two dotted lines are the bounds of ϕ. Points A' through D', J', and K' on the edge of disk D_R are set as in Case 2. However, on the edge of disk D_L, we set $H' = K'$ as shown in Fig. 10. We also set E', F', G' such that $\angle H'LG' = \angle G'LF' = \angle F'LE' = \frac{\pi}{3}$. Additional points S' and T' are set such that $\angle E'LS' = \angle D'RT' = \frac{\pi}{3}$. Two arcs $(T'R)$ and $(D'R)$ are made of points of unit distance from J' and C', respectively. We change the name of each area in $D_L \cup D_R$ as follows.

- Q_1: sector $(J'RA')$,
- Q_2: sector $(A'RB')$,
- Q_3: sector $(B'RC')$,
- Q_4^+: the shaded areas in $(C'RD')$,
- Q_6^+: the shaded areas in $(T'RJ')$,
- Q_5^+: $D_R \backslash \{Q_1 \cup Q_2 \cup Q_3 \cup Q_4^+ \cup Q_6^+\}$,
- Q_7: sector $(S'LE')$,
- Q_8: sector $(E'LF')$,

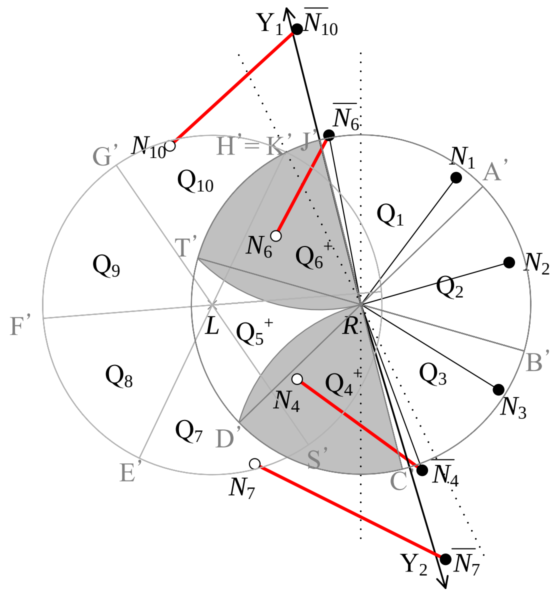

Fig. 10. Diagram of Case 4: $\phi_1 < \phi \leq \frac{\pi}{2}$.

- Q_9: sector $(F'LG')$,
- Q_{10}: sector $(G'LH')$.

Function $f(\cdot)$ and nodes $N_i, \bar{N}_i$ are defined as before.

We show $d(l^*) \leq 6$ by contradiction. Suppose that $d(l^*) = 7$. From $f(Q_5^+) = 0$, we should have $d(l^*) = f(Q_7, Q_8) + f(Q_9, Q_{10}) + f(Q_6^+, Q_1, Q_2, Q_3, Q_4^+) = 7$.

If $f(Q_7, Q_8) \leq 1$ and $f(Q_9, Q_{10}) \leq 1$, we have $f(Q_6^+, Q_1, Q_2, Q_3, Q_4^+) \geq 5$. We can show that $f(Q_7, Q_8) \leq 1$ and $f(Q_9, Q_{10}) \leq 1$ using the same approach as in Case 2 (see Fig. 8(b)). Then we must have $f(Q_6^+, Q_1, Q_2, Q_3, Q_4^+) \geq 5$. However, $f(Q_6^+, Q_1, Q_2, Q_3, Q_4^+) = 5$ leads to a contradiction to $\angle Y_1^* R Y_2^* < \pi$ from Lemma 8 and Fact 1 as in Case 3. Then, we can conclude that $d(l^*) \leq 6$.

It remains to show $f(Q_7, Q_8) \leq 1$ and $f(Q_9, Q_{10}) \leq 1$. To show $f(Q_9, Q_{10}) \leq 1$, it suffices to show that if $f(Q_9) = 1$, then $f(Q_{10}) = 0$. Assuming $f(Q_9) = 1$, we must have $\bar{N}_9 \in \hat{A}_R$. Let Z' denote the point on the extended line of (H', R) satisfying $\angle G'LZ' = \angle Z'LH' = \frac{\pi}{6}$. Similar to Case 2 in Fig. 8(b), we can show that $\overline{G'Z'} \geq 1$. Since $\angle LRY_1^* \geq \angle LRH' \geq \frac{\pi}{3}$, link $(N_9, \bar{N}_9)$ should intersects line segment (Z', H'), which implies that $f(Q_{10}) = 0$ from Corollary 2. Therefore, we can conclude that $f(Q_9, Q_{10}) \leq 1$.

Similarly we can show that $f(Q_7, Q_8) \leq 1$ as follows. Let H'' denote the point where D_L and D_R meets below line (L, R), and let Z'' denote the point on the extension of line (R, H'') such that $\angle H''LZ'' = \frac{\pi}{6}$.

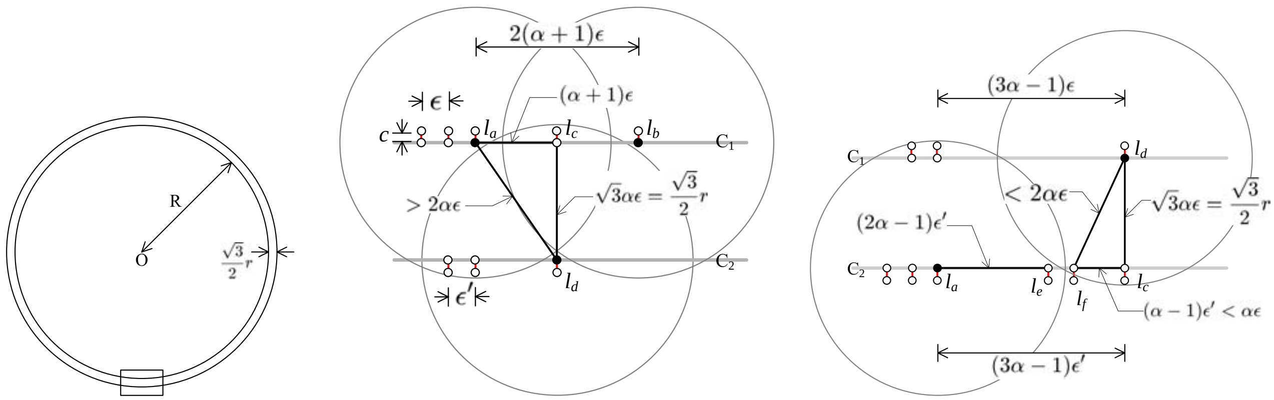

(a) Topology (b) An instance of $\vec{M}_i$; $\vec{\mu} \in Co(\{\vec{M}_i\})$ (c) An instance of $\vec{M}_j$; $\vec{\nu} \in Co(\{\vec{M}_j\})$

Fig. 11. A geometric network graph $G_K(V, E, I)$ and $\vec{\mu}, \vec{\nu} \in Co(\mathcal{M}_E)$ such that $\frac{1}{3}\vec{\mu} \succeq \vec{\nu}$. Figures illustrate the network graph and an instance of maximal schedules from $\vec{\mu}$ and $\vec{\nu}$, respectively. The interference range of some nodes (colored in black) are depicted.

Note that line (L, E') is parallel with line (R, Z''), and $\angle RLZ'' = \angle RLH'' + \angle H''LZ'' \geq \frac{\pi}{2}$. Then since Q_8 is on the left half plane of line (L, Z'') and Y_2 is on the right half plane of line (L, Z''), if $f(Q_8) = 1$, link $(N_8, \bar{N}_8)$ must intersect line (L, Z''). This implies that $f(Q_7) = 0$ from Corollary 2, which completes our proof of Case 4.

Considering all Cases 1 through 4, we conclude that $d(l^*) \leq 6$ for the left-most link l^* in a geometric unit-disc network graph under the 2-hop interference model.

D. Proof of Lemma 6

We prove the lemma by an example. After constructing a network graph, we find two maximal scheduling vectors such that one dominates the other with $\sigma \to \frac{1}{3}$.

We construct a network graph $G_K(V, E, I) \in \mathbb{G}_g^K$ as follows. On a circle C_1 at origin O, we place a set of nodes with an identical distance ϵ such that r is a multiple of ϵ, i.e., $r = 2\alpha\epsilon$ with an integer $\alpha > 0$. We denote the set of nodes by N_1. We also adjust the radius R of C_1 to be a multiple of $2\pi\epsilon$. We place another set of nodes, denoted by N_2, on another circle C_2 (at the same origin O) of radius $R + \frac{\sqrt{3}}{2}r$ as shown in Fig. 11(a). Each node in N_2 are aligned on a line with a node in N_1 and the origin O. Hence, nodes in N_2 are also placed with an identical distance ϵ', which is slightly larger than ϵ. Let $\Delta = \epsilon' - \epsilon > 0$. Note that Δ can be arbitrarily small by increasing R. For each node $n_i \in N_1$, we place another node n_j on a line of n_i and the origin O. The location of n_j is away from n_i *toward* O with distance $s(n_i, n_j) = c = \frac{r}{K-1}$. Let L_1 the set of links (n_i, n_j). For each node $n_p \in N_2$, we also place another node n_q on a line of n_p and the origin O. The location of n_q is away from n_p *out of* O with distance $s(n_p, n_q) = c$. Let L_2 the set of links (n_p, n_q). We can set $c \ll \epsilon$ by restricting $K > K_0$ with a large number K_0.

We first define the distance between two links $l_1 = (n_{1a}, n_{1b})$ and $l_2 = (n_{2a}, n_{2b})$ as the minimum distance between two nodes $n_x \in \{n_{1a}, n_{1b}\}$, and $n_y \in \{n_{2a}, n_{2b}\}$, and denote it by $S(l_1, l_2)$. That is, $S(l_1, l_2) := \min\{s(n_x, n_y) \mid n_x \in \{n_{1a}, n_{1b}\}, n_y \in \{n_{2a}, n_{2b}\}\}$.

We now find two maximal scheduling vectors $\vec{\mu}, \vec{\nu} \in Co(\mathcal{M}_{L_1 \cup L_2})$. Let $\vec{\mu}$ consist of a set of maximal schedules $\{\vec{M}_i\}$. An instance of $\vec{M}_i$ is shown in Fig 11(b), which is zoomed in the boxed area of Fig. 11(a). Suppose that two links $l_a, l_b \in L_1$ separated by $2(\alpha+1)\epsilon$ are included in a schedule. Let l_c denote the link in L_1 equally distant from l_a and l_b. Let l_d denote the link in L_2 that is aligned on a line with l_c and the origin O. Since $S(l_a, l_c) = S(l_c, l_b) = (\alpha+1)\epsilon > \alpha\epsilon$, and $S(l_c, l_d) = \sqrt{3}\alpha\epsilon$, we have $S(l_a, l_d) = S(l_b, l_d) > 2\alpha\epsilon = r$. Hence, link l_d can be scheduled along with l_a and l_b, and this pattern of active links repeats on the whole network graph. The set of maximal schedules $\{\vec{M}_i\}$ is obtained by shifting the pattern to right. It is clear that all links can be served for the same amount time during a unit time.

Let $\vec{\nu}$ consist of another set of maximal schedules $\{\vec{M}_j\}$. An instance of $\vec{M}_j$ is also shown in Fig. 11(c). Suppose that two links $l_a, l_b \in L_2$ separated by $2(3\alpha-1)\epsilon'$ are included in a schedule. Let l_c denote the link in L_2 equally distant from l_a and l_b. Let l_d denote the link in L_1 that is aligned on a line with l_c and the origin O. We show that if R is large enough and links $l_a, l_b \in L_2$, $l_d \in L_1$ are active, then no link in L_2 between l_a and l_b can be active. When the pattern of active links repeats, we can observe the same results on links between two active links in L_1. Due to bisymmetry at l_c, it suffices to show that all nodes between l_a and l_c are within an interference range either from l_a or from l_d. Let l_e and l_f denote links in L_2 that is away from l_a by $(2\alpha-1)\epsilon'$ and by $2\alpha\epsilon'$, respectively. If we increase the radius R such that $\Delta < \frac{\epsilon'}{2\alpha}$, then l_a interferes with l_e because $(2\alpha-1)\epsilon' < 2\alpha\epsilon$ but not with l_f. However, l_f interfere with l_d because the distance between l_f and l_d is less than $2\alpha\epsilon$ from $S(l_f, l_c) = (\alpha-1)\epsilon' < \alpha\epsilon$. Therefore, all links between l_a and l_c interfere with either l_a or l_d, and this pattern of active links repeats over the whole network graph. We compose $\vec{\nu}$ with maximal schedules that can be obtained by shifting the pattern to right. It is clear that all links can be served for the same amount time.

Since both $\vec{\mu}$ and $\vec{\nu}$ serve all links in $L_1 \cup L_2$ with the same amount of time, we can obtain σ such that $\sigma\vec{\mu} \succeq \vec{\nu}$ from the ratio of required time to equally serve all links. Let $T_{\vec{\mu}}$ and $T_{\vec{\nu}}$ be the required service time of $\vec{\mu}$ and $\vec{\nu}$, respectively. Assuming each link is served by a unit time, we have $T_{\vec{\mu}} = 2(\alpha+1)$ and $T_{\vec{\nu}} = 2(3\alpha-1)$ because all links between two active links in Fig. 11(b) and Fig. 11(c) should be served for a unit time. Hence, we obtain $\vec{\mu}, \vec{\nu} \in Co(\mathcal{M}_{L_1 \cup L_2})$ such that $\sigma\vec{\mu} \succeq \vec{\nu}$ with

$$\sigma = \frac{T_{\vec{\mu}}}{T_{\vec{\nu}}} = \frac{\alpha + 1}{3\alpha - 1}. \tag{6}$$

Hence, the local-pooling factor of G_K is less than σ, i.e., $\sigma^* \leq \frac{\alpha+1}{3\alpha-1}$. Note that we can increase α arbitrarily large by placing links closer and increasing the radius R. Therefore, we have some geometric graphs with $\sigma^* \rightarrow \frac{1}{3}$.

REFERENCES

[1] L. Tassiulas and A. Ephremides, "Stability Properties of Constrained Queueing Systems and Scheduling Policies for Maximal Throughput in Multihop Radio Networks," *IEEE Trans. Autom. Control*, vol. 37, no. 12, pp. 1936–1948, December 1992.

[2] X. Lin and N. B. Shroff, "The Impact of Imperfect Scheduling on Cross-Layer Congestion Control in Wireless Networks," *IEEE/ACM Trans. Netw.*, vol. 14, no. 2, pp. 302–315, April 2006.

[3] G. Sharma, C. Joo, and N. B. Shroff, "Distributed Scheduling Schemes for Throughput Guarantees in Wireless Networks," in *the 44th Annual Allerton Conference on Communications, Control, and Computing*, September 2006.

[4] X. Lin and S. Rasool, "Constant-Time Distributed Scheduling Policies for Ad Hoc Wireless Networks," in *IEEE CDC*, December 2006.

[5] E. Modiano, D. Shah, and G. Zussman, "Maximizing Throughput in Wireless Networks via Gossiping," *Sigmetrics Performance Evaluation Review*, vol. 34, no. 1, pp. 27–38, 2006.

[6] C. Joo and N. B. Shroff, "Performance of Random Access Scheduling Schemes in Multi-hop Wireless Networks," in *IEEE INFOCOM*, May 2007.

[7] A. Gupta, X. Lin, and R. Srikant, "Low-Complexity Distributed Scheduling Algorithms for Wireless Networks," in *IEEE INFOCOM*, May 2007.

[8] S. Sanghavi, L. Bui, and R. Srikant, "Distributed Link Scheduling with Constant Overhead," in *ACM Sigmetrics*, June 2007.

[9] C. H. Papadimitriou and K. Steiglitz, *Combinatorial Optimization: Algorithms and Complexity*. Prentice-Hall, 1982.

[10] B. Hajek and G. Sasaki, "Link Scheduling in Polynominal Time," *IEEE Trans. Inf. Theory*, vol. 34, no. 5, September 1988.

[11] S. Sarkar and L. Tassiulas, "End-to-end Bandwidth Guarantees Through Fair Local Spectrum Share in Wireless Ad-hoc Networks," in *IEEE CDC*, December 2003.

[12] P. Chaporkar, K. Kar, X. Luo, and S. Sarkar, "Throughput and Fairness Guarantees Through Maximal Scheduling in Wireless Networks," *IEEE Trans. Inf. Theory*, vol. 54, no. 2, pp. 572–594, February 2008.

[13] X. Wu and R. Srikant, "Scheduling Efficiency of Distributed Greedy Scheduling Algorithms in Wireless Networks," in *IEEE INFOCOM*, April 2006.

[14] G. Sharma, N. B. Shroff, and R. R. Mazumdar, "On the Complexity of Scheduling in Wireless Networks," in *ACM MOBICOM*, September 2006.

[15] E. Leonardi, M. Mellia, F. Neri, and M. A. Marsan, "On the Stability of Input-Queued Switches with Speed-Up," *IEEE/ACM Trans. Netw.*, vol. 9, no. 1, Feburary 2001.

[16] N. McKeown, "Scheduling Algorithms for Input-Queued Cell Switches," Ph.D. dissertation, University of California at Berkeley, 1995.

[17] A. Dimakis and J. Walrand, "Sufficient Conditions for Stability of Longest-Queue-First Scheduling: Second-order Properties using Fluid Limits," *Advances in Applied Probability*, vol. 38, no. 2, pp. 505–521, 2006.

[18] J.-H. Hoepman, "Simple Distributed Weighted Matchings," eprint, October 2004. [Online]. Available: http://arxiv.org/abs/cs/0410047v1

[19] V. S. A. Kumar, M. V. Marathe, S. Parthasarathy, and A. Srinivasan, "Algorithmic Aspects of Capacity in Wireless Networks," in *ACM Sigmetrics*, 2005.

[20] A. Brzezinski, G. Zussman, and E. Modiano, "Enabling Distributed Throughput Maximization in Wireless Mesh Networks: A Partitioning Approach," in *ACM MOBICOM*, 2006, pp. 26–37.

[21] G. Zussman, A. Brzezinski, and E. Modiano, "Multihop Local Pooling for Distributed Throughput Maximization in Wireless Networks," in *IEEE INFOCOM*, April 2008.

[22] R. Gallager and D. Bertsekas, *Data Networks*, 2nd ed. Prentice Hall, 1991.

[23] J. G. Dai, "On Positive Harris Recurrence of Multiclass Queueing Networks: A Unified Approach via Fluid Limit Models," *Annals of Applied Probability*, vol. 5, no. 1, pp. 49–77, 1995.

[24] M. J. Neely, E. Modiano, and C. E. Rohrs, "Power Allocation and Routing in Multibeam Satellites with Time-varying Channels," *IEEE/ACM Trans. Netw.*, vol. 11, no. 1, pp. 138–152, 2003.

[25] R. L. Cruz and A. V. Santhanam, "Optimal Routing, Link Scheduling and Power Control in Multi-hop Wireless Networks," in *IEEE INFOCOM*, San Francisco, April 2003.

[26] C. Joo, X. Lin, and N. B. Shroff, "Performance Limits of Greedy Maximal Matching in Multi-hop Wireless Networks," in *IEEE CDC*, December 2007.

[27] V. S. A. Kumar, M. V. Marathe, S. Parthasarathy, and A. Srinivasan, "End-to-end Packet-scheduling in Wireless Ad-hoc Networks," in *SODA*, 2004.

[28] H. Balakrishnan, C. L. Barrett, V. S. A. Kumar, M. V. Marathe, and S. Thite, "The Distance-2 Matching Problem and Its Relationship to the MAC-Layer Capacity of Ad hoc Wireless Networks," *IEEE J. Sel. Areas Commun.*, vol. 22, no. 6, pp. 1069–1079, August 2004.

[29] A. Israeli and A. Itai, "A Fast and Simple Randomized Parallel Algorithm for Maximal Matching," *Inf. Process. Lett.*, vol. 22, no. 2, pp. 77–80, 1986.

[30] C. Buragohain, S. Suri, C. Toth, and Y. Zhou, "Improved Throughput Bounds for Interference-aware Routing in Wireless Networks," in *COCOON*, 2007.